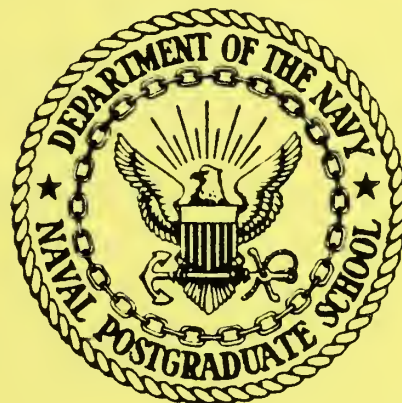


# NAVAL POSTGRADUATE SCHOOL

## Monterey, California



PERFORMANCE RATING OF ENHANCED  
MARINE CONDENSERS

by

R.H. Nunn  
P.J. Marto

August, 1982

Report for period ending 30 September 1982

Approved for public release; distribution unlimited.

Prepared for:

David Taylor Naval Ship R&D Center  
Annapolis, MD 21402

NAVAL POSTGRADUATE SCHOOL  
Monterey, California

J. J. Ekelund, RADM, USN  
Superintendent

D. A. Schrady  
Acting Provost

This report documents progress for the period ending 30 September, 1982, in the computer modelling portion of the project titled "Condenser Heat Transfer Augmentation."

The work reported herein has been monitored and supported by the David Taylor Naval Ship Research and Development Center, Code 2721, Annapolis, MD 21402.

Reproduction of all or part of this report is authorized.

This report was prepared by:

William M. Tolles  
Dean of Research

## UNCLASSIFIED

SECURITY CLASSIFICATION OF THIS PAGE (When Data Entered)

REPORT DOCUMENTATION PAGE		READ INSTRUCTIONS BEFORE COMPLETING FORM
1. REPORT NUMBER NPS69-82-005	2. GOVT ACCESSION NO.	3. RECIPIENT'S CATALOG NUMBER
4. TITLE (and Subtitle)  COMPUTER RATING OF ENHANCED MARINE CONDENSERS		5. TYPE OF REPORT & PERIOD COVERED Progress report for period ending 30 Sep 82
7. AUTHOR(s)  R. H. Nunn P. J. Marto		6. PERFORMING ORG. REPORT NUMBER
9. PERFORMING ORGANIZATION NAME AND ADDRESS Naval Postgraduate School Monterey, CA 93940		10. PROGRAM ELEMENT, PROJECT, TASK AREA & WORK UNIT NUMBERS 62543N; SF43400391 N00167-82-WR-0114
11. CONTROLLING OFFICE NAME AND ADDRESS DTNSRDC, Code 2721 Annapolis, MD 21402		12. REPORT DATE August, 1982
14. MONITORING AGENCY NAME & ADDRESS (if different from Controlling Office)		13. NUMBER OF PAGES 92
16. DISTRIBUTION STATEMENT (of this Report)		15. SECURITY CLASS. (of this report)  UNCLASSIFIED
17. DISTRIBUTION STATEMENT (of the abstract entered in Block 20, if different from Report)		
18. SUPPLEMENTARY NOTES		
19. KEY WORDS (Continue on reverse side if necessary and identify by block number) Heat transfer, Condenser, Enhancement, Computer modelling		
20. ABSTRACT (Continue on reverse side if necessary and identify by block number)  Condenser tubes with enhanced surfaces show promise for use in advanced marine condenser designs. In order to adequately predict the performance of enhanced tubes when operating in a condenser-bundle environment, considerable improvement in analytical method is necessary beyond the standard approaches recommended for use with conventional designs. This report describes a computer code of moderate complexity		

**UNCLASSIFIED**

~~SECURITY CLASSIFICATION OF THIS PAGE/When Data Entered.~~

that is suitable for predicting the relative merits of the use of enhanced tubes in radial-flow condensers. The code accounts for vapor shear effects, condensate inundation, and noncondensable gases, and predicts the local steam-side conditions at intermediate locations within the condenser bundle.

Several computer experiments are described in which the impacts of enhanced-tube designs on overall condenser performance are investigated. The results serve to illustrate the importance of internal detail in such analyses and, in addition, they show that judicious use of enhanced tubes can lead to considerable improvements in condenser performance as well as the realization of heretofore unattainable design options.

## SUMMARY

Condenser tubes with enhanced surfaces show promise for use in advanced marine condenser designs. In order to adequately predict the performance of enhanced tubes when operating in a condenser-bundle environment, considerable improvement in analytical method is necessary beyond the standard approaches recommended for use with conventional designs.

This report describes a computer code of moderate complexity that is suitable for predicting the relative merits of the use of enhanced tubes in radial-flow condensers. The code accounts for vapor shear effects, condensate inundation, and noncondensable gases, and predicts the local steam-side conditions at intermediate locations within the condenser bundle.

Several computer experiments are described in which the impacts of enhanced-tube designs on overall condenser performance are investigated. The results serve to illustrate the importance of internal detail in such analyses and, in addition, they show that judicious use of enhanced tubes can lead to considerable improvements in condenser performance as well as the realization of heretofore unattainable design options.

## TABLE OF CONTENTS

<u>INTRODUCTION</u> . . . . .	1
<u>EFFECTS OF LOCAL STEAM-SIDE CONDITIONS</u> . . . . .	4
LOCAL STEAM-SIDE PRESSURE VARIATIONS . . . . .	4
VAPOR VELOCITY EFFECTS ON STEAM-SIDE THERMAL RESISTANCE .	5
CONDENSATE INUNDATION . . . . .	8
NON-CONDENSIBLE GASES . . . . .	13
<u>SUMMARY</u> . . . . .	15
<u>COMPUTER MODELING</u> . . . . .	16
<u>THE MORCON COMPUTER CODE</u> . . . . .	19
DESCRIPTIVE SUMMARY . . . . .	22
Subroutine MAIN . . . . .	23
Subroutine SECALC . . . . .	26
Subroutine COOLEX . . . . .	28
Subroutine HETTRN . . . . .	28
Condensate Film Thermal Resistance . . . . .	30
Non-Condensable Gas Film Coefficient . . . . .	31
Subroutine PRSRDP . . . . .	34
SAMPLE RUN . . . . .	34
User Supplied Data . . . . .	36
Output . . . . .	41
RESULTS OF COMPUTER EXPERIMENTS . . . . .	43
<u>Effect of Internal and External Enhancement on     Bundle Length</u> . . . . .	43
<u>Variations in Thermal Resistance through the Bundle</u> . .	46
<u>Influence of Vapor Shear and Condensate Inundation</u> . .	49

TABLE OF CONTENTS  
(Continued)

<u>Enhancement in Bundles of Various Diameters</u> . . . . .	51
<u>SUMMARY</u> . . . . .	56
<u>CONCLUDING REMARKS</u> . . . . .	57
<u>LIST OF REFERENCES</u> . . . . .	59
Appendix A. MORCON Listing . . . . .	A1
Appendix B. Input Data Deck for Baseline Design . . . . .	B1
Appendix C. Summary and Detailed Output for Baseline Design . . . . .	C1
<u>INITIAL DISTRIBUTION LIST</u>	62



## PERFORMANCE RATING OF ENHANCED MARINE CONDENSERS

### INTRODUCTION

Since the early days of naval steam propulsion, the surface condenser has evolved into a very reliable component of the steam propulsion machinery plant. This reliability has been achieved by providing generous design margins to insure thermal performance at full power. The penalties for this overdesign, however, are additional weight and volume (which must be carried around for the life of the ship) and crowded machinery rooms with poor accessibility. Although surface vessels and submarines have different design constraints, both types of vessels can benefit from a more compact condenser design through improved heat transfer. The actual dimensions of the condenser may have an impact on vessel size and displacement, the location of the propulsion machinery aboard the vessel, and even on vessel performance and cost. In addition, the future development of compact steam systems, both for main propulsion and secondary heat recovery purposes, will require the application of advanced technology to all system components, including the condenser.

At the Naval Postgraduate School, the relative benefits of such advanced condenser designs have been analyzed using a modified, radial flow computer code (MORCON) to model the

heat transfer and fluid flow phenomena which occur within this type of heat exchanger. Refinements to this code and improvements in the models used to predict two phase heat transfer and pressure drop are continuing.

Based upon the work accomplished to date, it is clear that present day smooth-tube steam condensers, when operating under typical conditions, are limited in thermal performance due to a large thermal resistance which occurs on the sea-water side (tube side) of the condenser. This resistance, on the average, is larger than the thermal resistances which occur on the steam side and in the tube wall, and those due to seawater fouling and noncondensable gas buildup in the vicinity of the tube. Consequently, in present-day conventional condenser designs, what happens on the steam side does not have to be modeled too accurately to arrive at reasonable designs.<sup>1</sup> When using enhanced tubes, however, the enhancement on the sea-water side can increase the inside heat transfer coefficient by 100 to 200 percent over the smooth-tube case. The outside heat transfer coefficient, on the other hand, is increased by only 10 to 50 percent. In this situation, the thermal resistances on the inside and outside of the tube can be approximately equal. As a consequence, it becomes essential to understand and accurately model the detailed mechanisms which occur when steam condenses on these enhanced surfaces.

---

<sup>1</sup> It should be noted that, even with conventional designs, there can be locations within a condenser bundle where the steam side resistance is largest due to low vapor velocities and non-condensable gas pockets.

Heat transfer on the steam side of Naval condensers often occurs in the presence of high vapor velocities and with severe condensate inundation from neighboring tubes in the bundle. It is also important to predict the resulting two phase pressure drop in order to trace the steam flow path through the condenser bundle and minimize losses in the saturation pressure and temperature across the bundle. Since comprehensive test data on this subject are virtually nonexistent, and since advanced computer codes will depend strongly upon good steam-side models, additional experimental work is necessary.

In spite of the tentative nature of existing theoretical steam-side heat transfer models, it has proved to be useful to conduct computer-based condenser performance calculations in order to provide comparative information regarding the relative costs and benefits of enhanced-tube condensers. In addition, the present theoretical basis is adequate to permit the identification of condenser tube-bundle regions that should be particularly sensitive to the introduction of internal and/or external enhancement.

This report documents these computer-based calculations. Since steam-side conditions are especially important in such calculations, some preliminary discussion is devoted to this subject. This is followed by a brief general description of computer modelling of surface condensers. The computer code

used at NPS is then described and several case-studies are provided to illustrate the use of the code and to give some insights concerning the impact of enhanced-tube technology on condenser design.

#### EFFECTS OF LOCAL STEAM-SIDE CONDITIONS

Single-tube theories and experiments have shown, not surprisingly, that the thermal performance of a condensing tube may be dramatically affected by the thermo-fluid state of the surrounding two-phase multi-component flow. Thus the condensate loading and velocity of the vapor, its temperature, and its non-condensable gas content all have important influences on the thermal resistance on the steam side of the tube. These influences lead to further complications in the analysis of condenser tubes performing in a bundle environment and the overall bundle performance is strongly coupled to the bundle inlet conditions, individual tube performance, and the general nature of the tube distribution within the bundle. Several of the main factors that are likely to be significant in bundle performance are discussed in the following paragraphs.

#### LOCAL STEAM-SIDE PRESSURE VARIATIONS

Frictional pressure losses on the steam side of a condenser bundle are detrimental from a system point of view

because these losses are directly chargeable against the thermal efficiency of the power system. In addition, the vapor temperature, which is a major factor in the heat transfer process that accompanies condensation, is strongly dependent upon the pressure in the vapor. This dependency is accentuated at low condensing pressures, varying from about  $7^{\circ}\text{F}/\text{in. Hg}$  at 6 in. Hg condensing pressure to  $12^{\circ}\text{F}/\text{in. Hg}$  at 3 in. Hg. (In other words, at about 3 psia a loss of 0.1 psia in pressure will lead to a  $1.3^{\circ}\text{F}$  loss in vapor temperature and at 1.5 psia the loss would be about  $2.4^{\circ}\text{F}$ .) Consequently, when condenser tubes are closely packed in a bundle the resulting high vapor velocities and correspondingly high pressure losses can severely limit the bundle performance.

#### VAPOR VELOCITY EFFECTS ON STEAM-SIDE THERMAL RESISTANCE

High vapor velocities can have at least one effect that is beneficial. This is the shearing force that the vapor exerts on the condensate film which, at relatively high vapor velocities, can be significant. A number of investigators [1, 2, 3, 4] have contributed to the understanding of the effects of vapor shear. In particular, Fujii, et al. [1] have recently proposed experimental correlations of the form

$$\frac{Nu_m}{Nu_o} = C_1 \ Nu_o^{(4a - 1)} \ Re_L^{(.5 - 2a)} \quad (1)$$

where  $Nu_m$  is the mean Nusselt number,  $Re_L$  is the "two-phase" Reynolds number (based on vapor velocity, tube outside diameter, and kinematic viscosity of the condensate), and  $Nu_o$  is the standard Nusselt number for the ideal (zero shear) case. The empirical constants  $C_1$  and  $a$  are in the ranges

$$1.13 < C_1 < 1.24$$

$$.195 < a < .2$$

depending upon whether the tube thermal conditions are most appropriately described by constant temperature or constant heat flux conditions. The larger values are for the constant heat flux case. According to Fujii, et al., Eq. (1) is valid in the range  $3.3 > Re_L/Nu_o > 0.28$ . For smaller values of this parameter, they recommend the use of a slightly reduced value of the standard Nusselt number that is given by

$$Nu_m = 0.96 Nu_o$$

In a typical naval condenser, vapor velocities well above 100 ft/s are not uncommon and two-phase Reynolds numbers on the order of  $10^6$  are typical. For a nominal Nusselt number value of  $Nu_o = 400$ , the resulting vapor shear effect is given by  $Nu_m/Nu_o \approx 1.5$ . Thus, the vapor shear effect is clearly important in the range of operation of naval condensers, and, when enhancements of various kinds are applied, this effect may become a dominant factor in overall condenser performance predictions.

Correlations of the form of Eq. (1) appear to be adequate for the prediction of shell-side film coefficients in horizontal and downward vapor flow without condensate inundation. For upward vapor flow, however, the effects of vapor shear on film thickness appear to be much larger, and at very high velocities the shell-side film coefficient, normally low due to poor condensate removal, can be significantly increased - even to the extent that the influence of gravity is overcome by vapor shear effects.

From the point of view of enhancement, simple reasoning would lead to the expectation that improvements in heat transfer due to vapor shear will be less significant at high external enhancement conditions. This follows from the argument that enhanced tubes will carry thinner faster-moving condensate films (other conditions being equal) that are less sensitive to shearing effects acting at the vapor interface. Equation (1) reflects this effect in that (since  $a < .25$  in all known cases) the ratio  $Nu_m/Nu_o$  varies inversely with  $Nu_o$ . The vapor shear effect might also be reduced by some of the previously-mentioned external enhancement schemes employing extended surfaces that would trap or otherwise "protect" the condensate. With high levels of internal enhancement, on the other hand, failure to provide for adequate condensate removal will be somewhat compensated by the shearing of the relatively thick condensate film at high vapor velocities.

Other vapor velocity effects, such as rippling, induction of turbulence and stripping of the condensate film, are relatively poorly understood. A particularly important area in need of further research is the consideration of the entrainment of condensate droplets in fast-moving vapor flows. As will be discussed in the subsequent section, condensate droplets as they traverse the condenser can have a profound effect upon the performance of downstream tubes. To the extent that the paths of these droplets and the vapor flow are coupled through viscosity, an additional dependency upon vapor velocity must be considered.

#### CONDENSATE INUNDATION

The true behavior of the condensate generated within a tube bundle is far from the ideal model of vertically-dropping laminar sheets hypothesized by Nusselt. In fact, the condensate in most condenser environments will be in many forms (droplets, rivulets, sheets, sprays) and will flow in many directions. It is highly unlikely that any quantity of condensate will traverse a condenser without losing its identity by impinging upon other tubes in the bundle. The effect of this impingement is referred to here as condensate "inundation" or "rain" and it is probable that a true theoretical model of the phenomenon would of necessity be stochastic in nature. In the absence of such analytical sophistication, a

number of empirical models have been developed that are useful when applied within their range of credibility.

Strict application of the classical Nusselt theory, together with its restrictive assumption of a laminar film falling under the influence of gravity alone, leads to the conclusion that the average condensate film heat transfer coefficient for a vertical row of  $n$  tubes,  $\bar{h}_n$ , is given by [5]

$$\frac{\bar{h}_n}{h_o} = n^{-0.25} \quad (2)$$

where  $h_o$  is the single-tube film coefficient. Numerous investigators have compared this simple expression with experimental results [6, 7, 8, 9, 10, 11] and it has become clear that in reality the results obtained from Eq. (2) reflect an over-prediction of the detrimental effects of inundation. In fact, a modified form of Eq. (2) may be written as

$$\frac{\bar{h}_n}{h_o} = n^{-s} \quad (3)$$

where empirical evaluation of  $s$  has led to values in the range  $.07 < s < .25$  [7]. Within this range, for example, a column of 30 tubes may be judged to have an average film coefficient that is 79% to 43% of the single-tube value. It should be noted further that the actual film coefficient for the  $n$ -th tube in a column,  $h_n$ , may be found using Eq. (3) with the result that

$$\frac{h_n}{h_o} = n^{(1-s)} - (n-1)^{(1-s)} \quad (4)$$

The range of  $s$  leads to a range in  $h_n$  of from 75% to 32% of  $h_o$ : clearly the range of uncertainty in  $s$  is unacceptable.

Among the chief discrepancies in the assumed constancy in  $s$  in Eqs. (3) and (4) are:

1. The effect of inundation is definitely dependent upon the vapor velocity and direction.
2. Bundle tube layout (tube spacing and pattern) will influence condensate inundation.

Thus, even if the functional relationship given in Eq. (3) is authentic, the exponent  $s$  must show the dependency

$$s = fct (\text{steam velocity vector, bundle geometry}).$$

The first of these is indicated nicely by Brickell [11] in which a general decrease in  $s$  with steam velocity is shown. These results are reproduced here in Fig. 1. It is also apparent that at low steam velocities the exponent  $s$  is larger (more inundation effect) for both upward and downward steam flow than it is for horizontal steamflow. This directional effect is less noticeable at high steam velocities. The influence of tube separation upon inundation effects is not clearly discernable from available data, largely because of the coupling of vapor shear effects with those due to inundation. It is possible to speculate with some confidence, however, that closely-spaced tubes are more influenced by inundation than are the tubes in relatively disperse bundles.

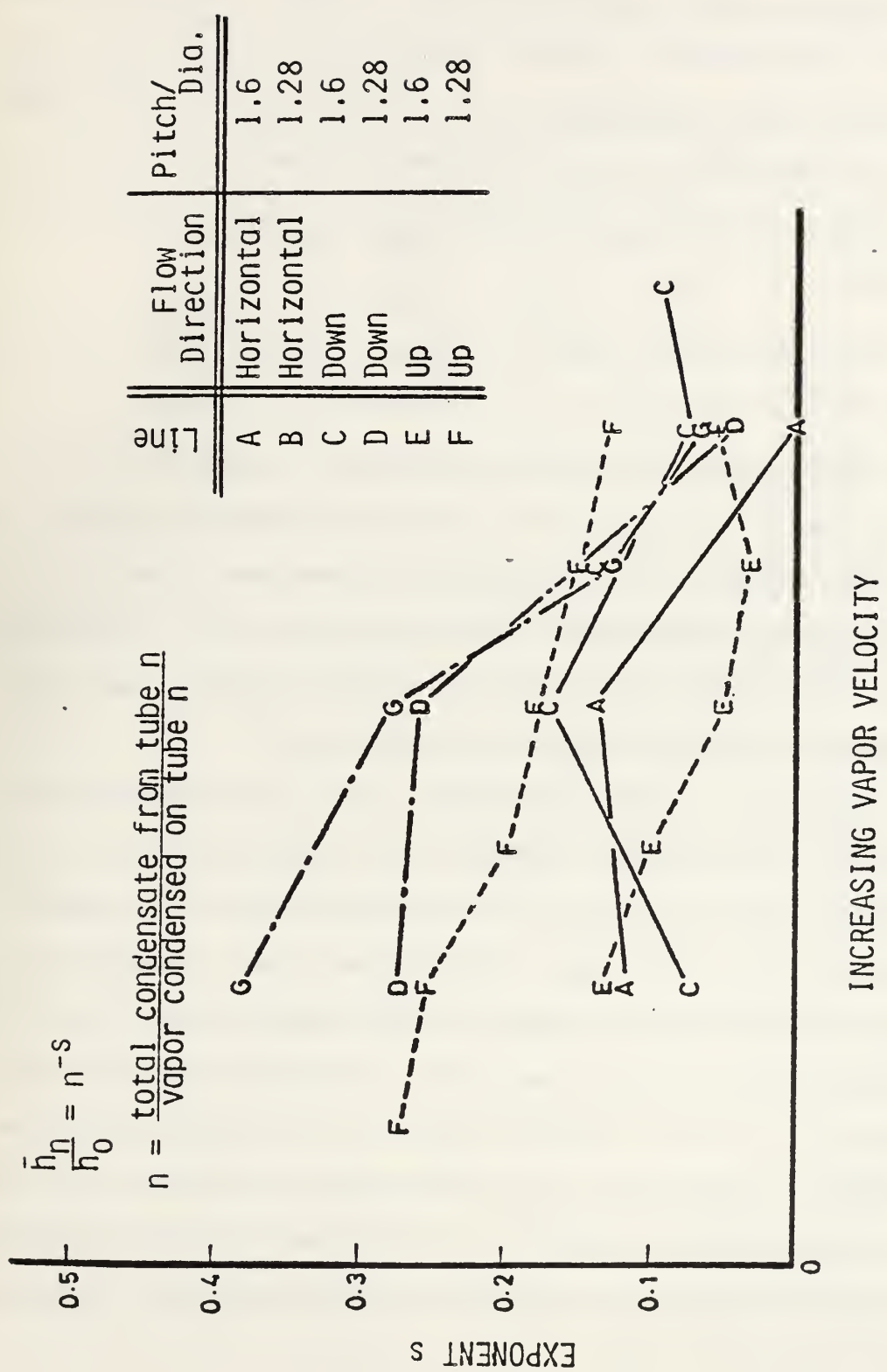


Figure 1. Effects of vapor velocity, flow direction, and tube spacing on tube performance in bundles[11].

One important influence of tube spacing in low velocity steam flow is that of side-drainage whereby condensate generated from above may, due to surface tension effects, proceeds laterally to adjacent tubes rather than directly downward. Eissenberg [7] has contributed a means of quantifying this effect with the result that Eq. (3) may be modified as follows:

$$\frac{\bar{h}_n}{h_o} = (1 - F_d)n^{-s} + F_d[0.6 + 1/2 (2n)^{-s}] \quad (5)$$

where  $F_d$  depends upon tube spacing and approaches unity for densely-packed staggered tube banks and zero for disperse tube layouts. Equation (5) represents the state-of-the-art in the prediction of condensate inundation effects and its effectiveness in doing so is, of course, highly dependent upon the selection of correct values for  $s$  and  $F_d$ .

The extent to which enhanced tubes are susceptible or resistant to inundation effects is a matter that is far from settled. (Indeed, the issue is unresolved as far as smooth tubes are concerned, when bundle effects are taken into account.) There are some experimental results [12] that indicate that smooth tubes operating in the dropwise mode of condensation are not greatly affected by inundation. (This observation was made at very low vapor velocities.) Preliminary indications are likewise encouraging for film condensation on enhanced tubes where single-tube experiments [13] have indicated values of  $s$  [Eq. (3)] in the range of 0.04 to 0.10.

## NON-CONDENSIBLE GASES

The effects of non-condensable gases can be classified into one of two categories:

1. The introduction of an additional local thermal resistance due to the propagation of gases towards a condensing tube surface under the influence of a gradient in partial pressure, and
2. The cumulative effect of gas blanketing where uneven rates of condensation in a condenser bundle eventually lead to regions where tubes are inoperative in a condensing role.

In naval condensers [14] as well as in shore-based power condensers [8], non-condensable gases contained in the inlet flow are usually on the order of 100-200 weight-parts-per-million. This ratio increases in the condenser, as steam is extracted, but even at a worst-case condition (20,000 wppm, say) the local overall heat transfer coefficient will be reduced by only about 15% and this in a very small region of the condenser. Thus, although a number of theories are available to account for the local effects of non-condensable gases [15] in naval condensers, there appears to be little need for extreme precision in the calculation.

The effect of non-condensable gases on the external resistance of enhanced tubes is a matter of considerable uncertainty. Cunningham [16] has recently reported on single-tube

experiments in which fine-finned tubes were found to be less affected by non-condensable gases than were smooth tubes under corresponding conditions. In any event, it is expected that because of the low concentrations of non-condensable gases under naval condenser conditions their effect will be small unless their presence in some way affects the enhancement process itself.

The more-important aspect of non-condensable gas effects, crucial in all condenser applications, is the design of tube bundles such that non-condensable gases do not accumulate. In large tube bundles it is often necessary to incorporate special inlet baffling and steam lanes that allow the steam to penetrate deep into all parts of the tube nest in order to avoid gas blanketing. The compensation of condenser bundle designs for this purpose has often been experimental in nature, involving large-scale and extremely expensive tests, and is probably a major reason why condenser cross-sections do not seem to change drastically from generation to generation.

In recent years, however, the ascendancy of computational capabilities has led to the feasibility of the comprehensive computer codes necessary for the prediction and alleviation of gas blanketing. One such computer code has been developed in the UK (such codes are not, in our experience, available to the public) and has been used to great advantage in the design and improvement of shore-based power condensers [8].

## SUMMARY

The performance of a condenser tube within a tube bundle is strongly influenced by the history of the vapor/gas mixture prior to arrival at the tube in question. Conversely, the performance of any given tube can have a profound effect upon the thermal behavior of tubes located downstream. The complexity of these interactions may lead to a degree of depression in the mind of the researcher who would predict overall bundle performance. On the other hand, these inadequacies in understanding may be viewed as challenges and, even in our present state of ignorance, we can answer questions in a relative way. For instance, qualitative trends due to augmentation may be identified and relative improvements due to augmentation may be quantified within a precision of perhaps 10-20%.

Just as a condenser is larger and more complex than a single tube, it is to be expected that the necessary computational and experimental scales will be larger for condensers than they are for single tubes. To justify such investments, and to guide the efficient allocation of resources, it is necessary to use what tools we have at hand to investigate potential payoffs and pacing problems. The following sections describe some preliminary results obtained from computer models of condenser bundles.

## COMPUTER MODELING

Analytical models for the estimation of condenser performance may be classed as follows:

1. Standard methods of the "black-box" type that are used for preliminary - and sometimes, it is suspected for final - design purposes. These methods include those recommended by the Heat Exchange Institute (HEI [17]) and British Electrical and Allied Manufacturers' Association (BEAMA [18]).
2. Intermediate computer codes that, to varying extents, include the details of tube-to-tube flow within the condenser. For purposes of classification, these codes are restricted to the analysis of condenser designs in which the vapor/gas mixture may be presumed to flow in a fixed direction (such as radial, horizontal, upwards, or downwards). The code MORCON is of this class and is described in some detail below.
3. Multi-dimensional codes utilizing finite element or finite difference methods for the solution of the governing conservation equations. Because codes in this category are proprietary (in all cases, to our knowledge), little is known concerning the extent to which they exist and work. The CERL code mentioned above [8] appears to be quite successful in application

and there are some indications [19] that U.S. manufacturers possess a similar capability.

The black-box methods are extremely limited to their application to all but the most standard condenser designs. In essence, only the overall heat transfer coefficient,  $U$ , is predicted by these methods and even this is subject to considerable uncertainty (HEI predictions of  $U$  have been observed to differ from measured values by from 100% on the high side to 50% on the low side [20]). These methods of prediction are based upon the assumption that the overall thermal resistance is dominated by the internal (tubeside) resistance - they are limited to cases of moderate cooling water velocity - and the allowances for fouling are subject to considerable criticism on physical bases. No means are provided for accounting for the distribution of thermal resistances across individual tube sections or between tubes in a bundle. It is clear that major advances in condenser designs cannot be based on these black-box methods.

At the other extreme of the spectrum of sophistication lie the multi-dimensional computer-based methods. The basic computational difficulties in the development of these comprehensive computer codes are largely ones of scale. It is quite difficult, yet most important to include two-dimensional capabilities that allow calculations in the plane of flow normal to the axis of the condenser. The third dimension,

steam/gas flow in the direction of the tube axis, may be obtained with reasonable accuracy by combining two-dimensional slices. Even so, the complexity of the two-dimensional calculation is sufficient unto itself in that it is often necessary to compute the two-phase multi-component flow in the passages between thousands of tubes. As a result, it is common to combine groups of tubes into "mini-bundles". Within these mini-bundles the equations of mass, momentum, and energy are satisfied by means of finite-difference expressions for the convective, conductive, and source effects. The source terms in these expressions require much of the approximation necessary in less-complicated codes in terms of interaction effects such as vapor shear and condensate inundation. Thus, the extension to multi-dimensional computations does not obviate the need for additional insights into the various bundle interactions mentioned in the previous section. The chief benefit of such extensions appears to be the ability to predict the performance of poorly designed condenser bundles especially with respect to air-blanketing.

Multi-dimensional computer codes can be extremely valuable for condenser performance predictions and may even be essential to the development of truly optimized condensers. Large resource investments are required for the development of such codes and questions inevitably arise concerning their cost-effectiveness. This issue is not developed further here except to say that, because of it, our emphasis has been at the

intermediate level of analytical sophistication where codes such as MORCON are found.

#### THE MORCON COMPUTER CODE

MORCON (Modified Oak Ridge Condenser) is a modified version of the ORCON1 code developed at the Oak Ridge National Laboratories [21]. Some of the features and limitations of MORCON are summarized below:

- a. MORCON allows the calculation of radial flow in circular bundles. (Other unmodified versions of ORCON1 have been developed for downward and horizontal-flows.)
- b. Correction of the condensate film coefficient for the effects of rain, including side drainage, is accomplished by the means previously described. As has been pointed out, the correction only accounts for the distribution of condensate rain upon lower tubes in a gravity-dominated flow and does not account for the interaction of vapor shear effects with those due to inundation.
- c. Non-condensable gases (up to four species) are taken into account by the use of the Colburn analogy [22] together with an empirical correlation credited to Eissenberg in [21].
- d. MORCON allows for the effects of heat transfer enhancement of the inner and/or outer film coefficients. The influence of enhancement on tubeside and shell-side pressure drops is also included.

- e. MORCON, as in all other known cases, includes fouling effects only as a constant resistance term.
- f. All tube-side and shell-side fluid properties are continuously calculated as they change with pressure and temperature throughout the condenser. The latter quantities vary due to inlet, outlet, and tube-to-tube flow cross-section variations, as well as viscous losses.
- g. Bundles can be segmented into as many as six computational sectors. Steam flow entering each sector is adjusted until the shell-side pressures at the exits of each sector (which is also the air cooler inlet) are matched within a specified limit. The sector arrangement for the circular bundle with radial flow is illustrated in Fig. 2.
- h. The overall heat transfer coefficient for each row in each sector is calculated on the basis of an "average" tube. This is a basic limitation of the code that is somewhat relieved by the ability to calculate performance by sectors.
- i. Vapor shear effects are included in the manner previously described. To the extent that the Fujii correlation does not include the interaction of vapor velocity with condensate inundation, the results are suspect for other than gravity-dominated (low vapor velocity) flow.

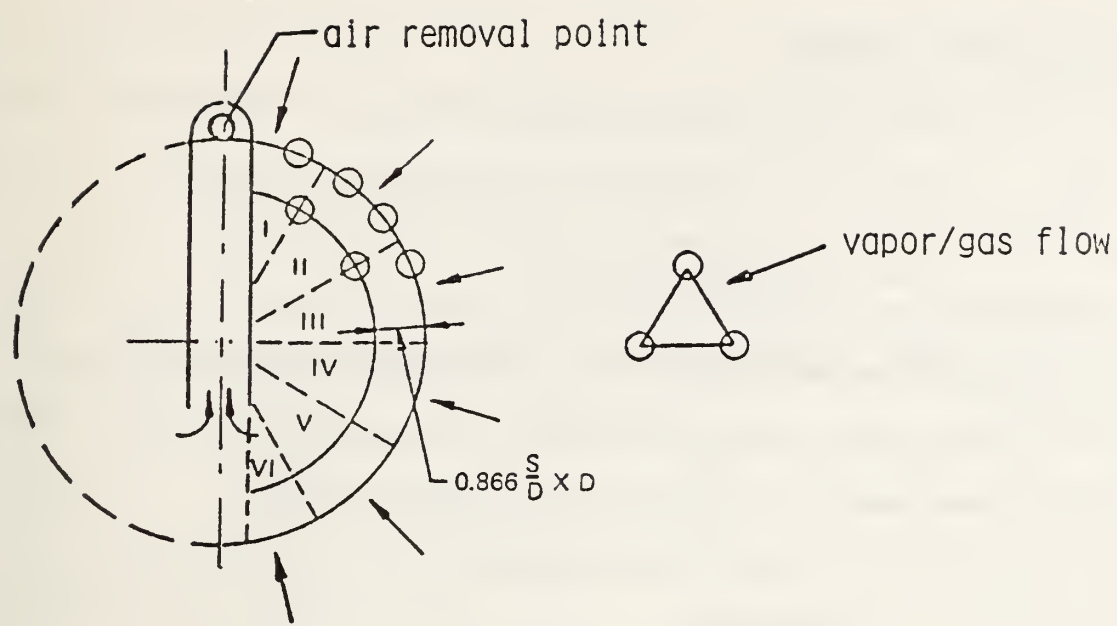
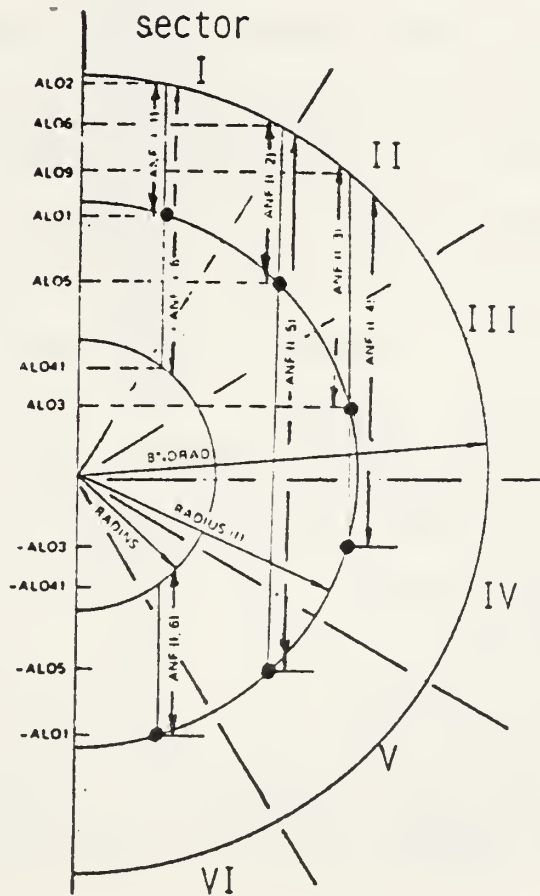


Figure 2. Sketches showing sector arrangements and quantities necessary for inundation calculations [21].



## DESCRIPTIVE SUMMARY

In this section the organization and flow of MORCON are described. A listing of the code is provided in Appendix A. Because MORCON is in large part identical to the ORCON1 code, the treatment here will be brief with details confined to the few modifications made to ORCON 1. For a more complete description of the basic code, the reader is referred to [21]. The subroutines contained in the code are listed below:

MAIN (not labeled)

SECALC

COOLEX

HETTRN

ADJUST

PRSRDP

DFSVTY

INPUT

OUTP1

ZERO

Subroutine DFSVTY computes the mutual diffusivity of the vapor/gas mixture. Various function subroutines are included to calculate specific heats, thermal conductivities, viscosities, and densities of the gas, vapor, and condensate as required. Function subroutines are also provided to calculate vapor saturation pressures and temperatures and the latent heat of vaporization. The purposes of subroutines INPUT, OUTP1, and ZERO are indicated

by their names and these will receive no further discussion here. The subroutine calling protocol is indicated in Table I, below.

Table I. Subroutine Calling Protocol

Calling Sub- Routine	Called Subroutine							
	SECALC	COOLEX	HETTRN	ADJUST	DFSVTY	PRSDRP	INPUT	OUTPL
MAIN	X	X		X			X	X
SECALC			X			X		
COOLEX			X			X		
HETTRN					X			

#### Subroutine MAIN

Subroutine MAIN is the main control program. Input values are taken into this subroutine and the tube bundle cross-sectional geometry is determined. This geometry is defined by the specified number of tubes, their outside diameter, and the spacing between them. The tubes are arranged radially such that the outer row of the bundle is complete. The tube array is staggered with the radial spacing between rows equal to  $(\sqrt{3}/2)$  times the specified circumferential spacing between tubes. The void diameter is determined by the space necessary to accommodate the number of tubes that are insufficient to complete an outer row. With the tube sheet entirely filled (zero void diameter), the specification of additional tubes will result in the removal of a number of tubes from the void sufficient to complete an additional outer row. (Because of the difference in performance of inner and outer-row

tubes, this method of allocating tube cites leads to highly non-linear and sometimes confusing results when tube count is used as an independent design variable.)

Bundle symmetry is assumed about the vertical centerline of the circular bundle and the remaining semi-circular tube array is divided into six sectors. Each partial row in each sector is defined by the central tube in that string and the program calculates the number of tubes in a vertical row above this "mean" tube. This is needed to provide for inundation calculations.

Following these preliminary arrangements, subroutine SECALC is called. The return information is the condition of the vapor/gas mixture as it leaves the main condenser bundle and enters the air cooler. The performance of the cooler is then computed by means of a call to subroutine COOLEX.

The final overall vapor/gas conditions, as returned from COOLEX, are transmitted to subroutine ADJUST. If the exit fraction of the current design is equal to the input specification (within five percent error) the return from ADJUST is followed by final output actions. If the specified exit fraction is not obtained, the code will adjust either the inlet steam flow or the tube (bundle) length, as selected by the user. The updated design is then returned to SECALC for evaluation and the above procedure is repeated until convergence is obtained or the iteration limit (set to 10) is exceeded.

Figure 3, below, summarizes the function of subroutine MAIN.

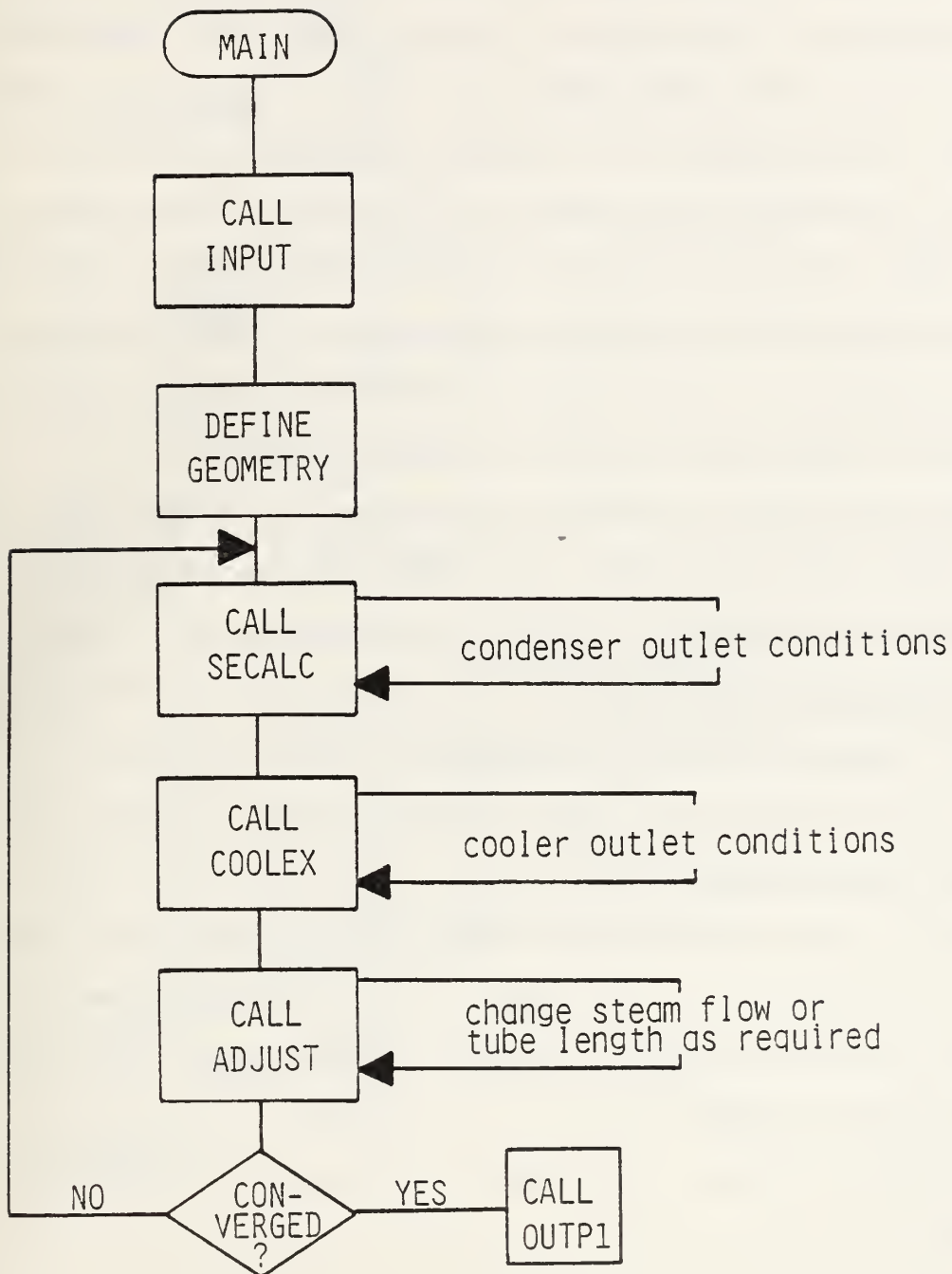


Figure 3. Simplified flow diagram of main calling subroutine.

### Subroutine SECALC

Subroutine SECALC, with calls to subroutine HETTRN, determines the sector-by-sector and row-by-row performance of the condenser. Calculation is begun in the first (uppermost) sector at the first (outermost) row. Using the central tube of this and subsequent row segments, subroutine HETTRN is called to determine the thermal performance of the current "man" tube. With information returned from HETTRN, subroutine PRSDRP is called to determine the pressure of the vapor/gas mixture entering the next row and the steam quantity and conditions for this next row are returned to HETTRN.

The outer loop in SECALC covers the six sectors while the inner loop covers the rows (the number of rows is determined by the input geometry). Following the completion of both loops, the steam-side pressures at the outlet of each sector are each compared with the mean of the outlet pressures. The total inlet steam flow is then adjusted so that sectors with excessive steam-side pressure drop receive less flow and conversely for those sectors with relatively higher outlet pressures. The calculation is then repeated in its entirety (all sectors, all rows) until the bundle outlet pressure is uniform to within one percent.

Figure 4, below, illustrates the function of subroutine SECALC.

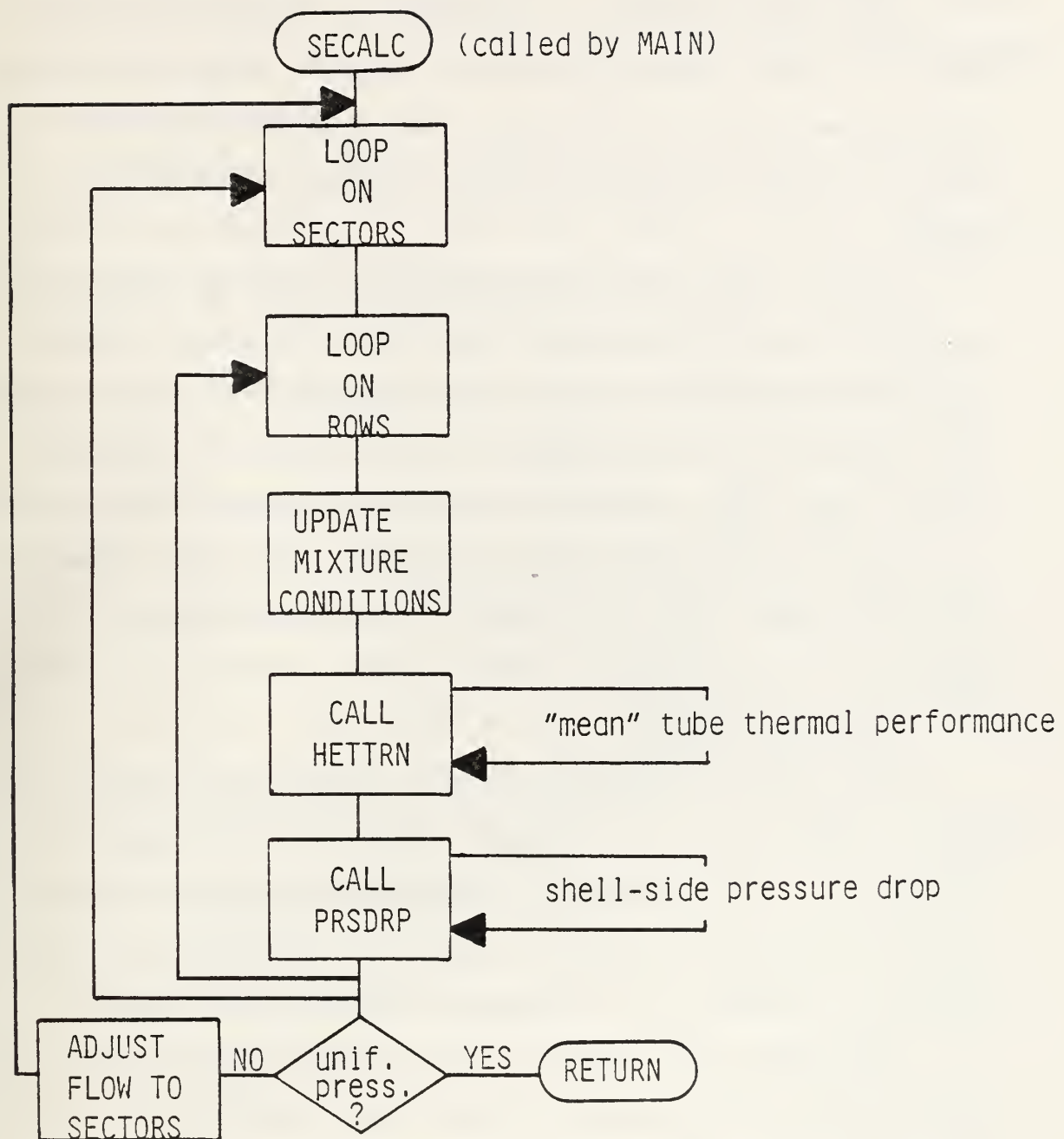


Figure 4. Simplified flow diagram for subroutine SECALC.

### Subroutine COOLEX

Subroutine COOLEX is a simplified version of subroutine SECALC in which calls to HETTRN are used to obtain row-by-row performance of the cooler tubes. No steam-side pressure balance (such as that performed in SECALC) is attempted in COOLEX.

The user specifies the percentage of the total number of condensing tubes to be used in the cooler section. These tubes are allocated to a vertical staggered array with cross-flow dimension initially equal to the bundle void diameter. If this tube cite allocation results in crowding of the cooler tubes (as indicated by vapor/gas mixture velocities in excess of 150 ft/s) the cooler is widened (and proportionately shortened) as necessary.

### Subroutine HETTRN

This program contains the basic heat transfer algorithms and, as noted above, is called by SECALC for each mean tube in each row of each sector. Following a summary of the procedures followed in HETTRN, a few of the more-important heat transfer algorithms are discussed in some detail below.

Because the thermodynamic and physical properties of the cooling water are allowed to depend upon temperature in HETTRN, a basic iteration is required to compute the overall heat transfer coefficient. This iteration begins with an estimate from which, with local steam conditions and cooling water inlet

temperature and flow rate, the cooling water outlet temperature is calculated. Cooling water properties are then calculated based upon the mean of the inlet and outlet temperatures of the cooling water.

Following the determination of cooling water properties, HETTRN then computes, in order, the internal thermal resistance (based upon the Dittus-Boelter correlation with internal enhancement taken into account) and the external condensate film thermal resistance based upon the Nusselt correlation (see below). The external resistance is then corrected for vapor shear and condensate rain effects. These resistances, together with tube conduction resistance and a constant fouling resistance (input by the user), are then summed to develop an interim value of total resistance to heat transfer, exclusive of the resistance of the non-condensable gas film. The thermal resistance of the non-condensable gas film is calculated and various key variables for the current iteration are determined. Convergence of the basic loop is based upon agreement between current and previous values of film temperature drops. Agreement to within 0.01 degrees Fahrenheit is required in the case of the liquid film temperature drop and if non-condensable gases are present the iterations continue until the calculation of the gas film temperature drop is steady to within 0.001 degrees Fahrenheit. Following convergence, values are transferred to SECALC and common storage as necessary for future use.

### Condensate Film Thermal Resistance

In MORCON the standard Nusselt relationship for the condensate film resistance is corrected for vapor shear effects according to the correlations of Fujii et al. [1]. On the assumption that the thermal resistance on the steam side is relatively small, the constant heat flux case is taken to be most appropriate. (Within experimental uncertainties the two cases - constant heat flux or uniform wall temperature - are not appreciably different.) Eq. (1) becomes

$$\frac{Nu_m}{Nu_o} = 1.24 \ Nu_o^{-0.2} \ Re_L^{0.1} \quad (6)$$

where  $Nu_o$  is the Nusselt relationship given by

$$Nu_o = 0.725 \left[ \frac{g\sigma^2 d^3 h_{fg}}{K_L \mu_L \Delta T} \right]^{1/4} \quad (7)$$

Following correction of the mean Nusselt number for vapor shear effects, this value is further corrected for condensate inundation. Equation (5) is applied with a value of  $s = 0.2$  so that the average film coefficient for a vertical row of  $m$  tubes is given by

$$\frac{\bar{h}_m}{h_0} = 0.6F_d + (1 - 0.5647F_d)^{-0.2} \quad (8)$$

This expression is evaluated for  $m = n$  and  $m = n-1$ , where  $n$  is the number of condensing tubes vertically above the

tube in question, and the heat transfer coefficient for that tube is given by

$$h_n = n \bar{h}_n - (n-1) \bar{h}_{n-1} \quad (9)$$

The selection of the exponent  $s = 0.2$  in these calculations is based upon the comparison with experiment shown in Fig. 5 and is also in consonance with the observations of others [7, 11, 23] (see also Fig. 1).

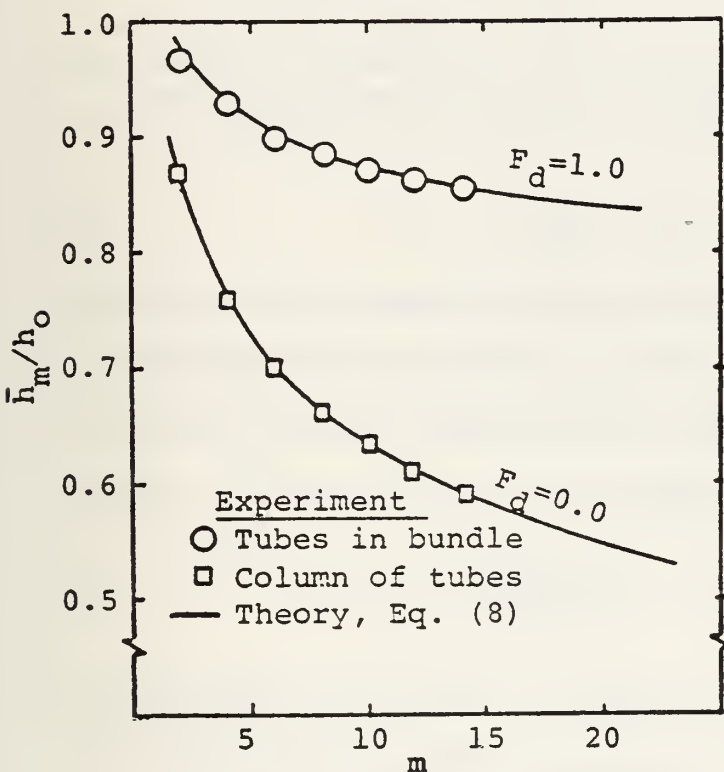


Figure 5. Tubes with inundation and side drainage; comparison of theory with experiment. Data of Ferguson and Oakden ("Heat Transfer Coefficients for Water and Steam in a Surface Condenser," Trans. Chem. Eng. Congress (World Power Conf.), v.3; 640 (1936)) as reported in [7].

#### Non-Condensible Gas Film Coefficient

The process of heat transfer through the non-condensable portion of the gas/vapor mixture is modelled as one due to mass transfer of the vapor through the gas. Sensible heat

transfer across the gas film (usually about 0.1% or less) is neglected. A mass transfer coefficient,  $K_G$ , is defined such that

$$K_G = \frac{h_g \Delta T}{h_{fg} \Delta P_{sf}} = \frac{h_g}{h_{fg}} \left( \frac{\partial T}{\partial P} \right) \quad (10)$$

where  $\Delta P_{sf}$  is the drop in vapor partial pressure in the film,  $\Delta T$  is the corresponding temperature change,  $h_{fg}$  is the latent heat of vaporization, and  $h_g$  is the heat transfer coefficient for the process across the non-condensable film.

The drop in vapor partial pressure across the gas film is taken equal to the rise in gas partial pressure across the film so that

$$\Delta P_{sf} = P_{gc} - P_{gb} \quad (11)$$

where  $P_{gc}$  and  $P_{gb}$  are the gas partial pressures at the condensate film interface and the external mixture conditions, respectively. Combining Eqs. (10) and (11), the gas film temperature drop may be written:

$$\Delta T = \frac{K_G h_{fg}}{h_g} P_{gc} - P_{gb} \left( \frac{\partial T}{\partial P} \right) \quad (12)$$

The partial pressure  $P_{gb}$  is known at each point in the calculation and the rate  $(\partial T / \partial P)$  is calculated from the saturated steam line. The condensate interface gas partial pressure is taken from the empirical relationship suggested by Eisenberg and Noritake [24]:

$$P_{gc} = \frac{C_j}{K_G}$$

where

$$C_j = \frac{G}{(S_c)^{2/3}} \exp (.54 - .544 \ln Re)$$

with  $G$  the local mass velocity,  $S_c$  the local Schmidt number, and  $Re$  the local vapor Reynolds number. With this correlation, Eq. (13) becomes

$$\Delta T = \frac{C_j h_{fg}}{h_g} - P_{gb} \left( \frac{\partial T}{\partial P} \right) \quad (13)$$

The gas film temperature drop may be further defined in terms of heat transfer coefficients by the following heat balance:

$$h_g \Delta T = U_g \Delta T_m \quad (14)$$

where  $U_g$  is the overall heat transfer coefficient belonging to the log-mean temperature difference  $\Delta T_m$ . That is, if  $U$  is the heat transfer coefficient without non-condensable gases (known, at this point in the calculation) then:

$$\frac{1}{U_g} = \frac{1}{h_g} + \frac{1}{U} \quad (15)$$

Combination of Eqs. (13) - (15) with the elimination of  $\Delta T$  and  $h_g$  leads to the following quadratic relationship for the overall heat transfer coefficient:

$$U_g^2 - \left\{ \frac{h_{fg} C_j}{\Delta T_m} + U \left[ 1 + \frac{P_{gb}}{\Delta T_m} \left( \frac{\partial T}{\partial P} \right) \right] \right\} U_g + \frac{h_{fg} C_j U}{\Delta T_m} = 0 \quad (16)$$

All the quantities necessary to determine the coefficients in this relationship are available (for the current iteration) so that a solution for  $U_g$  is forthcoming. Solutions for  $h_g$  and  $\Delta T$  follow according to Eqs. (15) and (14).

Subroutine PRSRDP

As the name implies, the purpose of this subroutine is to compute the pressure drop on the steam side between adjacent rows of tubes. In MORCON (as in ORCON1) the friction factor is given by [24]:

$$f = 0.102 + \frac{52.2}{Re} \quad (17)$$

where  $f$  is related to the pressure drop by

$$\frac{4f}{\frac{1}{2} \rho v^2} = \Delta P$$

or

$$\Delta P = \frac{2fG^2}{\rho}$$

The application of the correlation of Eq. (17) is limited to moderate mass velocities ( $G < 1500 \text{ lb/hr - ft}^2$ ) and, as such, may lead to significant errors when used to predict steam-side pressure drops in some advanced marine condenser designs.

SAMPLE RUN

In this section a sample run is described in order to illustrate the necessary user procedure and to provide a baseline case for subsequent analysis of the effects of enhancement. The tubesheet layout for the baseline design is shown in Fig. 6.

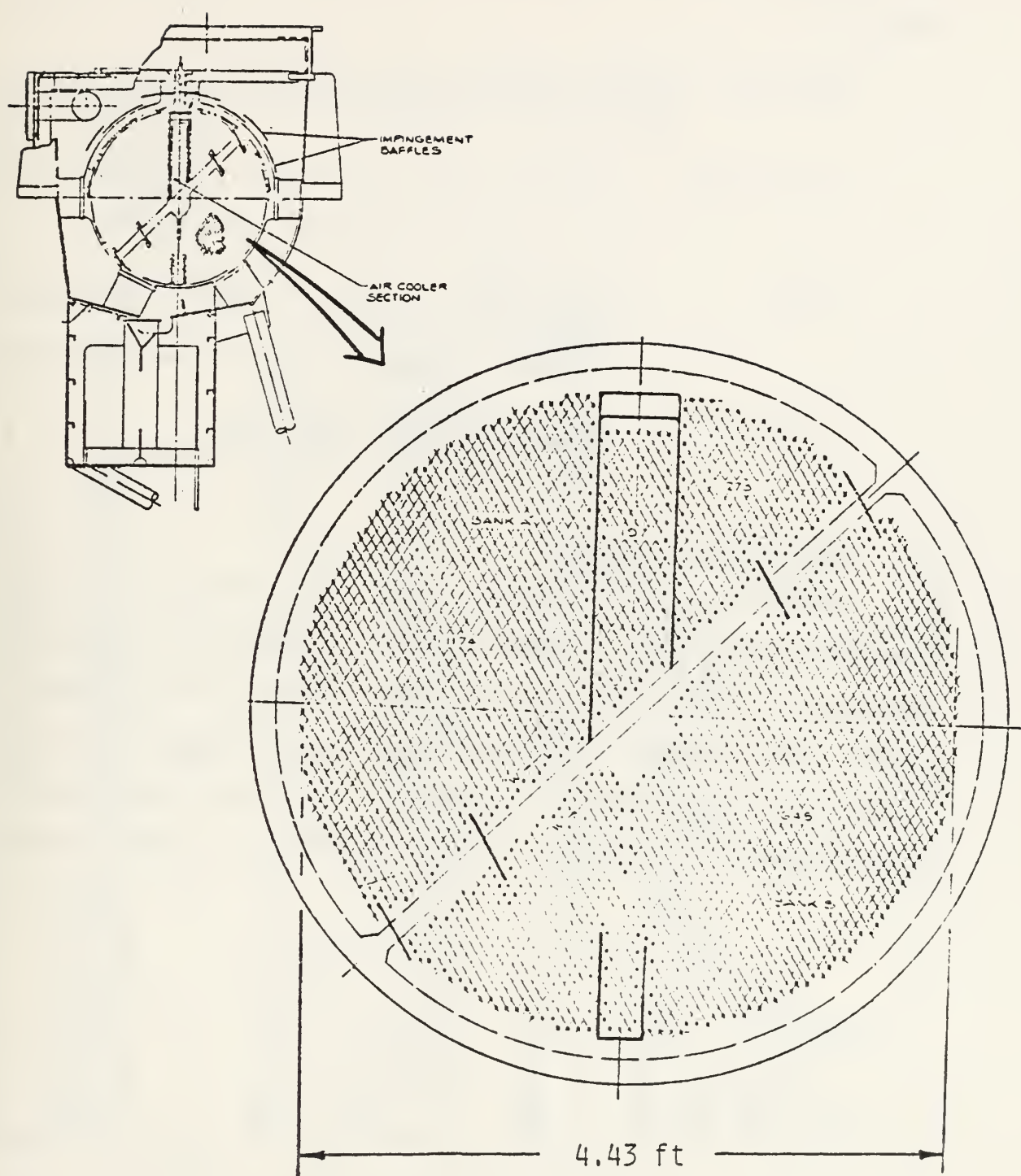


Figure 6. Assembly and tubesheet layout for baseline condenser.

and general specifications for this design are listed in Table II.

Table II. Design and Performance Specifications for the Baseline Condenser

Inlet steam: 189,003 lb<sub>m</sub>/hr saturated 5 in.Hg (133.7°F)

33.7 lb<sub>m</sub>/hr noncondensibles (air)

Tubes: 1646 tubes in each of two passes, 6% in cooler  
70-30 Cu Ni, 5/8 OD, 16 BWG (0.065 wall)  
Pitch/OD 1.35  
Fouling Resistance  $3.3 \times 10^{-4}$  hr ft<sup>2</sup> °F/Btu

Cooling water: Inlet temperature 66.1°F  
Velocity 8 ft/s (7,900 gpm)  
Salt concentration 3.5% by weight

#### User Supplied Data

Subroutine INPUT reads, writes, and processes the data provided by the user. These data are supplied via seven cards, as illustrated in Fig. 7. The first five of these cards are identical to those described for ORCON1 [21] but the input nomenclature is repeated here so that the reader may proceed (it is hoped) without reference to that document.

CARD 1 (11, 19A4, A3)

A2	10	20	30	40	50	60	70	80
----	----	----	----	----	----	----	----	----

## CASE IDENTIFICATION

CARD 2 (7F10.0, 21S)

ANTP	PRCCLR	SDD	SDDMIN	OD	50	XW	60	NRWSD	NRWSCP
------	--------	-----	--------	----	----	----	----	-------	--------

CARD 3 (6F10.3)

WBI	VELBI	CBI	STBI	FOUL	ENWI
10	20	30	40	50	60

CARD 4 (5A1, 7F5.2, 4I5)

GAS	SEC	FEC	HFC	RAG	FLG	FLM	FDAVE	EXTI	PUT	PU	INSTM	ITRAN	OAT	IPNCH
5	10	15	20	25	30	35	40	45	50	55	60			

CARD 5 (6F10.3)

WSI	WNCI	STSAT1	ALST	ENHO	ENHI
10	20	30	40	50	60

CARD 6 (4F10.3)

ENHFI	TUBESW	FC	FEXP
10	20	30	40

CARD 7 (2I5)

IRAIN	IVAP
5	10

Figure 7. Card deck layout for input data.

Following is a list of definitions of the input parameters. A listing of the input cards for the baseline case is given in Appendix B (compare Table II).

Card 1, (FORMAT: I1, 19A4, A3)

IR Indicator for cards to be read (column 1 only). If IR = 0, 4, or >5, then all seven cards will be read in proper order.

INDENT All the remaining columns of the first card are available for identification or notes, 79 columns

Card 2, (FORMAT: 7F10.0, 215)

ANTP Total number of tubes in the bundle (includes cooler).

PRCCLR Percent of tubes in the cooler.

SDD Ratio of tube circumferential center-to-center spacing to tube diameter

SDDMIN Ratio of tube spacing to tube diameter for cooler section.

ØD Outside diameter of all tubes, in.

XW Wall thickness of tubes, in.

SKW Thermal conductivity of tube material, Btu/hr-ft<sup>2</sup>-°F/ft.

NRWSP Number of rows of condenser coolant inlet temperatures to be read (use only to read punched card inlet coolant temperatures, set = 0 otherwise).

NRWSCP Same as NRWSP except for cooler.

Card 3, (FORMAT: 8F10.3)

WBI Total coolant flow to condenser (cooler included), lb/hr.

VELBIP Coolant velocity, ft/sec.

(Note: WBI and VELBIP are exclusive variables; one of them should be set to zero. If not, then VELBIP will override WBI).

CBI Coolant salt concentration, fraction by weight.

STBIP Coolant inlet temperature, °F.

(Note: STBIP is used only if inlet coolant temperatures are not read in or transferred.)

FOUL Tube fouling resistance hr-ft<sup>2</sup>-°F/Btu

ENHI Tube internal heat transfer enhancement factor.

Card 4, (FORMAT: 5A1, 7F5.2, 4I5)

GAS Type of noncondensable gas, must be one of AIR, CO<sub>2</sub>, or MIX.

SECFLG Bundle model indicator, gives number of 30° sectors in one-half of a symmetrical bundle, or total sectors in a semicircular bundle.

HFCDFL Symmetry indicator.

If = 1, model will have symmetry about a vertical centerline

If = 0, model will be a semicircular type.

RADFLG Factor to increase bundle radius beyond that normally calculated by the code (will enlarge center void).

BAFFLE Flag to indicate presence of baffles at 2  
and 4 o'clock.

FDAVE Tube spacing parameter. Used in subroutine  
HETTRN to modify effect of condensate flood-  
ing.

EXITFR Target value for vented steam as a percent of  
input. If EXITFR = 0.0, then program will  
make a single pass and return the results  
without any adjustments.

ØUTPUT Control flag to restrict amount of detail  
printed out.

ØUTPUT = 1.0 gives full detail of all sectors.  
ØUTPUT = 0.0 prints only summary.

INSTM Flag to direct program flow when converging on  
exit fraction (EXITFR) target.

INSTM = 1, inlet steam adjusted.  
INSTM = 0, tube length adjusted.

ITRAN Flag to direct code to use outlet coolant tem-  
peratures from immediate preceding run (used  
only when multiple stages are run together)  
for inlet temperatures of current stage.

ITRAN = 1, use transferred temperatures  
ITRAN = 0, do not use transferred temperatures.

IFLTAT Flag to give option of having detail output in  
floating point form; one gives floating point,  
zero gives fixed point.

IPNCH     Outlet coolant temperatures will be punched  
            for input if IPNCH = 0.

Card 5, (FORMAT: 8F10.3)

WSI     Steam flow to condenser, lb/hr.

WNCI     Noncondensable gas flow to condenser, lb/hr.

STSAT1     Inlet steam temperature,  $^{\circ}$ F

ALST     Tube length, ft.

ENHØ     Tube external thermal enhancement factor for  
            heat transfer.

ENHF     Friction factor enhancement factor for use in  
            calculation of pressure drop in the steam.

Card 6, (FORMAT: 4F10.3)

ENHFI     Friction factor enhancement factor for cooling  
            water pressure drop

TUBESW     Specific weight of tube material, l /ft.<sup>3</sup>

FC     Coefficient for enhanced-tube friction factor  
            formula of the form  $f_{cw} = FC * (Re_{cw}/10^5)^{**FEXP}$

FEXP     See FC

Card 7, (FORMAT: 2I5)

IVAP,     Switches to control vapor shear and inundation  
IRAIN     effects. If set less than one these effects  
            are neglected.

#### Output

Subroutine OUTP1 handles the principal output from the run. First, an image of the input deck is reproduced followed by an expanded version of this information. There next follows a series of statements defining the progress of the iterations

to achieve the specified exit fraction. In the baseline case (Appendix C) the tube length is successively adjusted until convergence is achieved in the ninth iteration. There follows a table of data describing the condenser, cooler, and overall performance. Next, average inlet and outlet coolant temperatures are calculated for the condenser and the cooler. From these averages overall log mean temperature differences, DTCND2, DTCOL2, and DLTOT2, are calculated for the condenser, cooler and overall, respectively, using inlet steam temperatures. For the appropriate values of heat removed, the overall heat transfer coefficients, UPCOND, UPCOOL, UPAVG, are found for the condenser, cooler, and entire bundle. In addition, during the run, a row-by-row average of the heat transfer coefficients (UBARW, UBARWC, UAVGW, respectively) is made, and the corresponding log mean temperature differences (ADTCND, ADTCLR, ADTOA, respectively) are back calculated.

The option exists to print only the summary of results (OUTPUT = 0), or to have the summary plus two pages of detailed results for each sector (OUTPUT = 1). In the event of an error condition existing when the output subroutine is entered, the above calculations will be omitted and only the detailed output will be printed.

Appendix C contains the summary output as well as the detailed output. In addition, a listing of definitions (not normally included) is inserted to facilitate the analysis of the detailed output. At the bottom of the summary output

(preceding the detailed output) are seven additional quantities. These are defined as follows:

BUNL2P	Tube length for two-pass bundle, ft
BUNVOL	Bundle volume, including tubes and voids, ft <sup>3</sup>
BUNWT	Bundle weight, lb
RETUB	Cooling water Reynolds number
FRIFAC	Cooling water friction factor
HDLOSS	Cooling water head loss, ft H <sub>2</sub> O
PMPPWR	Cooling water pumping power, hp

#### RESULTS OF COMPUTER EXPERIMENTS

The following calculations examine applications of the MORCON code to departures from the baseline design. Several computer experiments are described in order to demonstrate some of the effects of internal and external enhancement of tubes contained within bundles. In addition, these examples serve to illustrate some of the influences that tube-to-tube interactions can have upon the performance of tubes in bundles.

##### Effect of Internal and External Enhancement on Bundle Length

Figures 8a and 8b illustrate the predicted effect of internal and external enhancement in terms of the length of tubes necessary to maintain the baseline heat duty. Constant heat duty is obtained by iteratively varying the tube length to obtain a fixed exit fraction of 0.05% of the baseline inlet

steam flow. Figure 8 includes manufacturer's data for enhancement factors of some commercially available augmented tubes and it is seen that combined internal and external enhancement can be expected to lead to bundle length (and volume and weight) reductions on the order of 35%. Table III gives information describing the augmented tubes used in this study.

Table III. Characteristics of Some Commercially-Available Augmented Tubes<sup>1</sup>

Tube	Groove Geometry		Thermal Enhancement Factors		Head Loss Factor <sup>2</sup>
	Pitch Dia	Depth Dia	Internal	External	
KL	0.543	0.025	2.14	1.05	2.03
KM	0.543	0.040	2.51	1.14	3.26
YL1	0.250	0.013	1.44	1.35	1.56
YL2	0.250	0.013	1.44	1.94	1.47
YM1	0.125	0.0215	2.70	1.38	6.02
YM2	0.125	0.0215	2.70	1.94	5.69

Notes:

1. Tubes KL and KM are products of Wolverine Division, UOP Inc. [25]. Tubes YL1, YL2, YM1, and YM2 are products of Yorkshire Imperial Metals, LTD [26].
2. Figures shown are ratios of head loss values to the smooth-tube case for the baseline conditions.

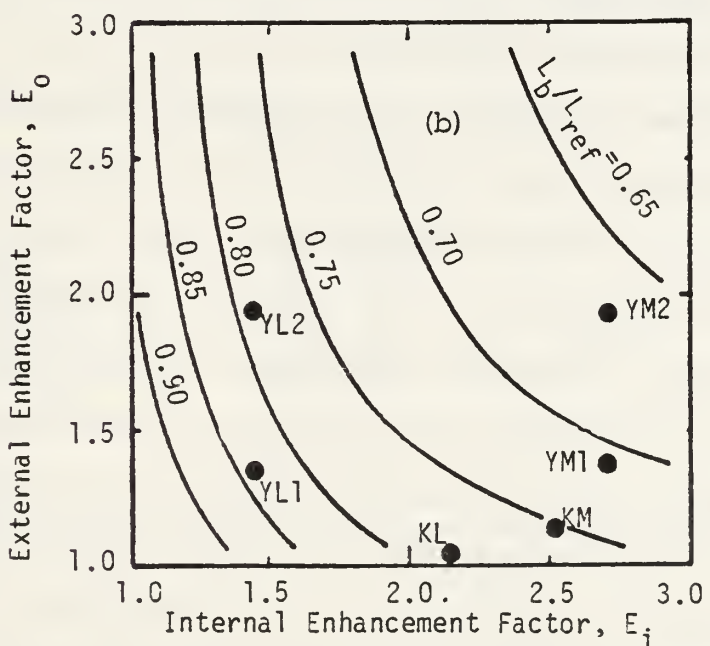
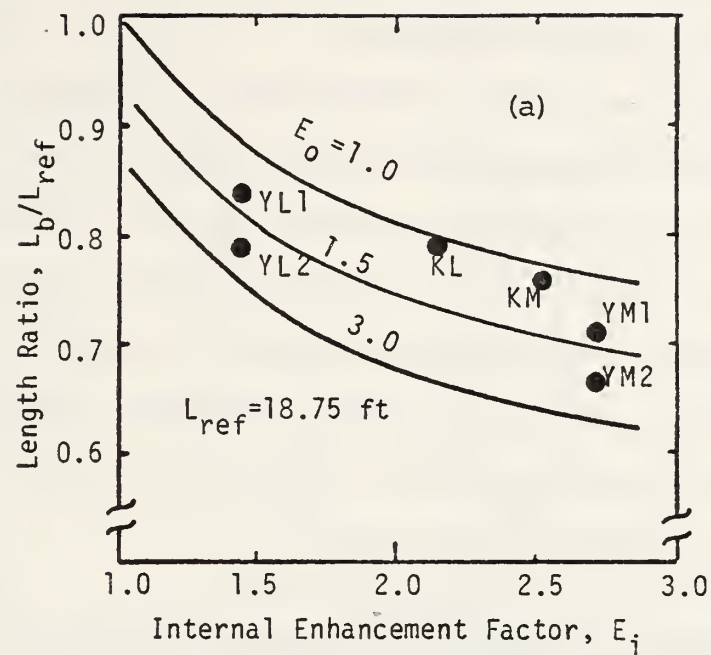


Figure 8. Effects of internal and external enhancement on tube length; baseline condenser.

The smooth-tube baseline is, as is typical, controlled in thermal resistance by the tube side film coefficient. For this reason internal enhancement is relatively more effective (about 2:1) than external enhancement. Figure 8b is a cross-plot of Fig. 8a and indicates the combinations of internal and external enhancement necessary for a given length reduction. Here again it is seen that internal enhancement is justifiable to large values relative to external enhancement or, by way of example, external enhancement beyond 1.5 may not be warranted unless the internal film coefficient is enhanced by a factor of at least 2.

#### Variations in Thermal Resistance through the Bundle

The importance of considering the limiting thermal resistance is further illustrated in Figs. 9a and 9b. Figure 9a illustrates the row-by-row variation in internal and external resistances for a condenser with no external enhancement. Without internal enhancement, the thermal circuit is unbalanced (dominated by the internal resistance) throughout the condenser. External enhancement in this case would clearly be gilding the thermal lily. With an internal enhancement of 2.0, however, the two film resistances are relatively balanced. Such would be the approximate case for the KL tube of Fig. 8.

If external enhancement is to be applied, on the other hand, such as in the case of YM1 in Fig. 8, additional internal

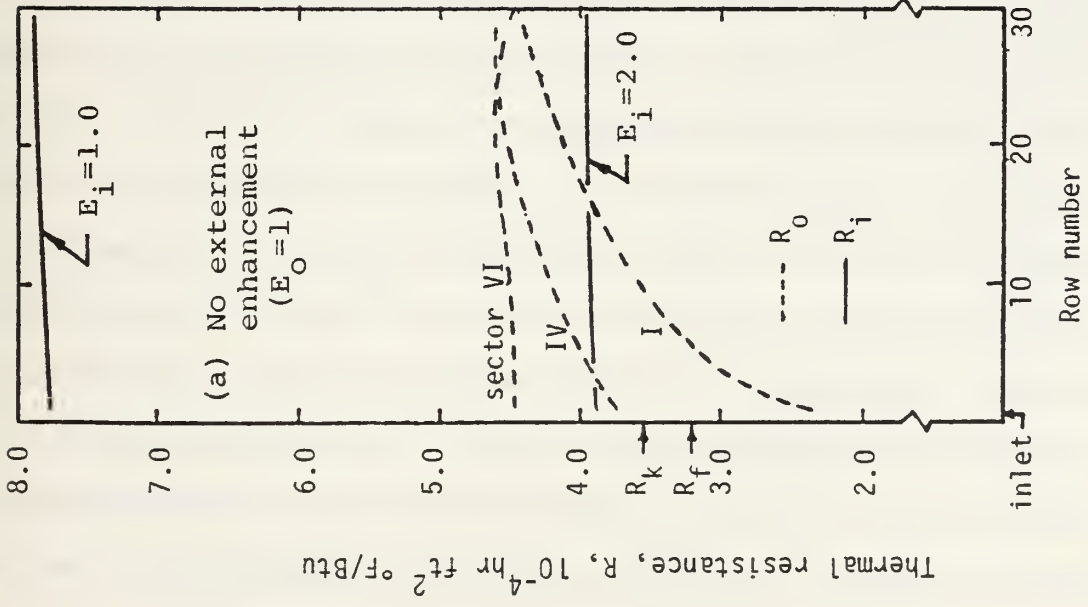
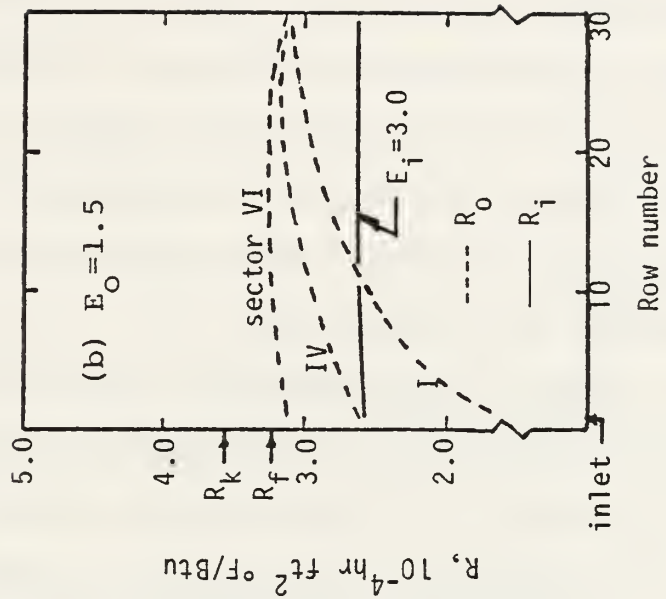


Figure 9. Row-by-row variations of thermal resistances.



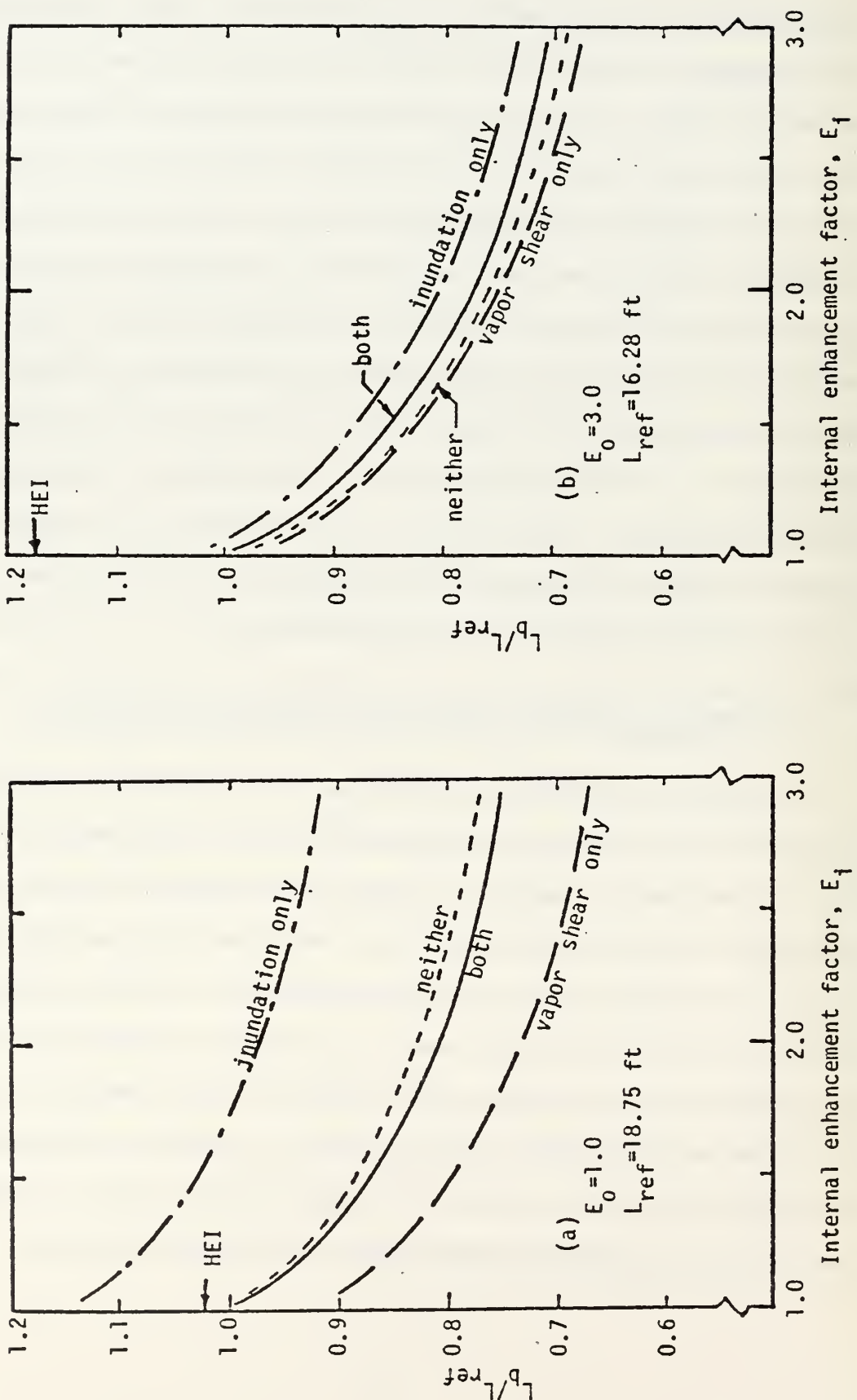
enhancement is to be recommended. Such a case is illustrated in Fig. 9b where, again, the relative balance is obtained between the two film resistances by using an inside enhancement of  $E_i = 3.0$  and an outside enhancement of  $E_o = 1.5$ . It should be noted that in Fig. 9b the film resistances have been lowered below the thermal resistances due to fouling ( $R_f$ ) and tube wall resistance ( $R_k$ ) (resistance due to the non-condensable gas film is negligible in this case). Therefore, further improvements would be most noticeable from reduction in  $R_f$  and/or  $R_k$ .

Figures 9a and 9b also illustrate the complicated nature of the shellside resistance. The dashed lines indicate the distribution of external resistance in sectors I, IV, and VI of the condenser, with sector I at the top of the bundle (center ray at  $15^\circ$ ) and proceeding clockwise in  $30^\circ$  increments to sector VI. In sector I a procession radially inward from row 1 to row 30 is in the direction of gravity and each successive row is inundated by the row above - thus the continuous increase in  $R_o$  in sector I. In sector VI, however, each row radially inward is subject to less inundation so that a general improvement is realized from the point of view of condensate inundation. In every sector, however, the vapor velocity is decreasing in a radially inward direction and the beneficial effect of vapor velocity is correspondingly less in regions toward the center of the bundle. In the top

sector (sector I) condensate inundation and vapor shear effects change in the same direction with resistance increasing radially inward. In the bottom sector (sector VI) the inundation and vapor shear change oppositely and there is a general balance. It will be noted that near the bundle exit (entrance to the air cooler section) in sector VI the decreases in vapor shear effects no longer overcome the changes due to reduced inundation and the resistance begins to decrease. Sector IV is also illustrated in these figures and is seen to represent something of a mean behavior among the sectors. The spread between sectors in the external resistance,  $R_o$ , is seen to be reduced in Fig. 9b because of reduction in the relative effect of vapor shear with external enhancement.

#### Influence of Vapor Shear and Condensate Inundation

Figures 10a and 10b illustrate the potentially deceptive nature of the influence of vapor shear and condensate inundation in condenser bundles. Figure 10a examines the relative influence of the two effects upon required tube length and their dependency on internal enhancement. In this case the favorable effect of vapor shear is roughly balanced by that of inundation and in terms of required bundle length they are by no means independent of each other. Without enhancement the two effects are essentially equivalent so that the HEI method, which neglects them both, appears to be adequate (for



rather serendipitous reasons). With enhancement, however, when row-by-row thermal performance must be considered, the neglect of either vapor shear or condensate inundation can lead to erroneous results (e.g., the neglect of vapor shear would indicate no improvement with an internal enhancement of about 1.7). Figure 10b shows that when external enhancement is large, these effects are less important because of the dominance of thermal resistances other than those due to the shellside film.

#### Enhancement in Bundles of Various Diameters

The number of possible comparisons such as those shown here is virtually limitless. As a final example, it might be useful to illustrate some of the influences to be expected with enhancement when the number of tubes in the bundle and hence the bundle diameter is allowed to vary. Figures 11a-11f illustrate this effect for a range of internal enhancement factors with no external enhancement (Figs. 11a-11c) and with  $E_o = 3.0$  (Figs. 11d-11f). In each set of figures the changes in bundle length, volume, and weight are shown for variations of  $\pm 20\%$  in the number of tubes in the bundle with the cooling water velocity held constant at 8.0 ft/sec. The reader will draw his own conclusions but a few interesting points may be highlighted here.

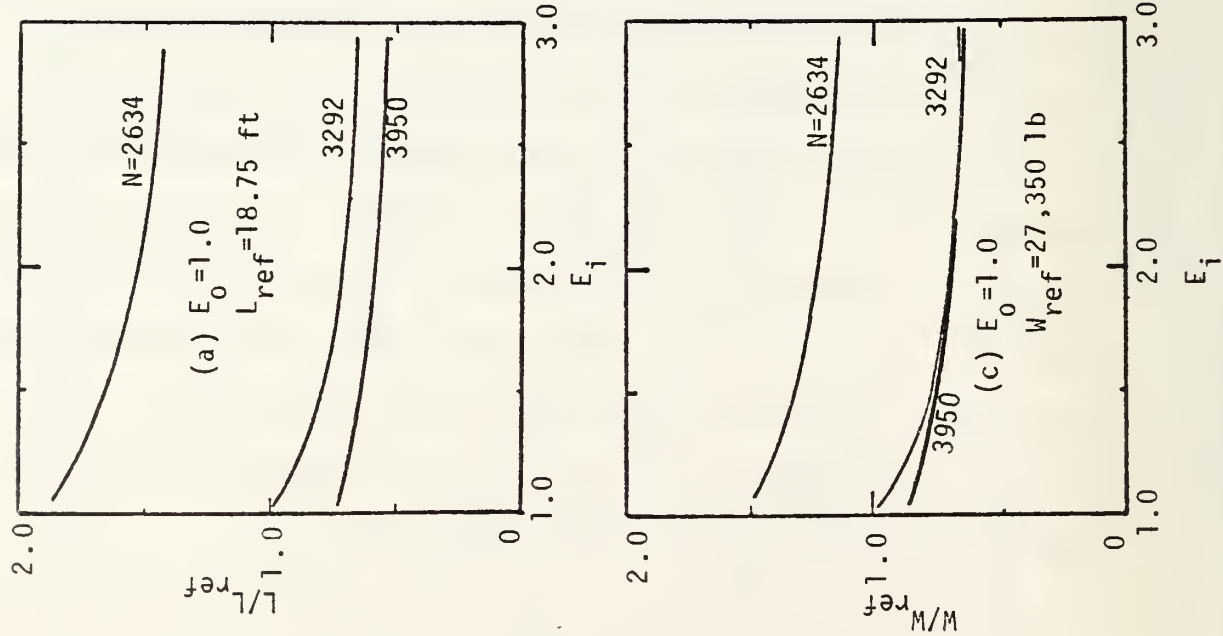
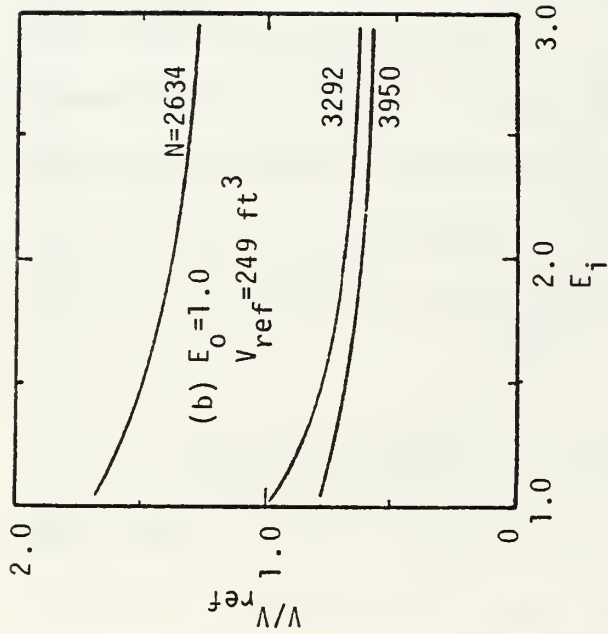


Figure 11. Variations of bundle length, volume, and weight. Baseline heat duty with cooling water velocity of 8 ft/s;  
 (a)-(c) no external enhancement.



number of tubes $N$	bundle diameter ft.
2634	3.73
3292	4.15 (baseline)
3950	4.57

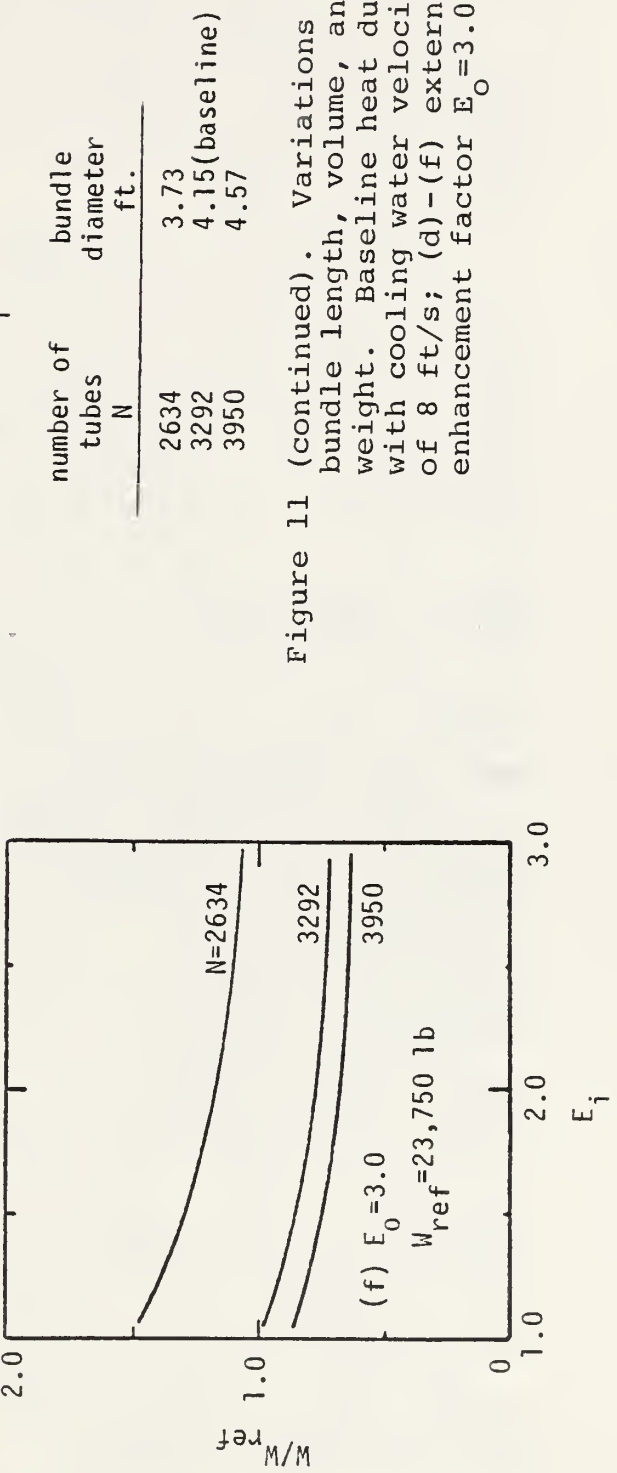
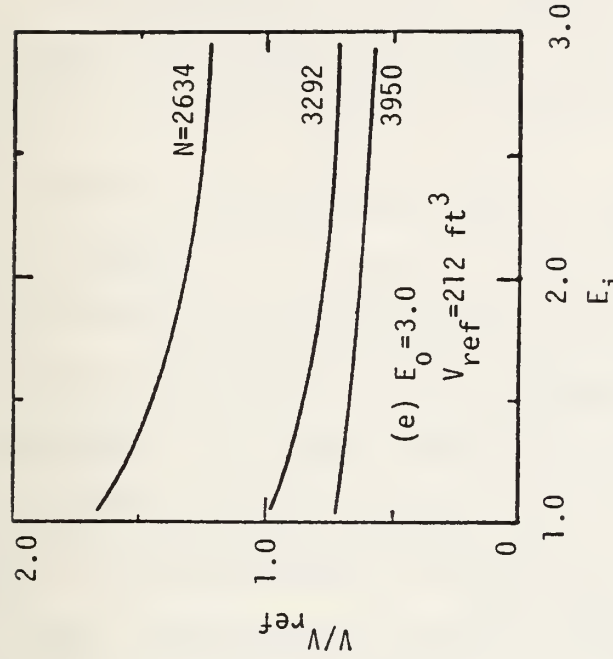
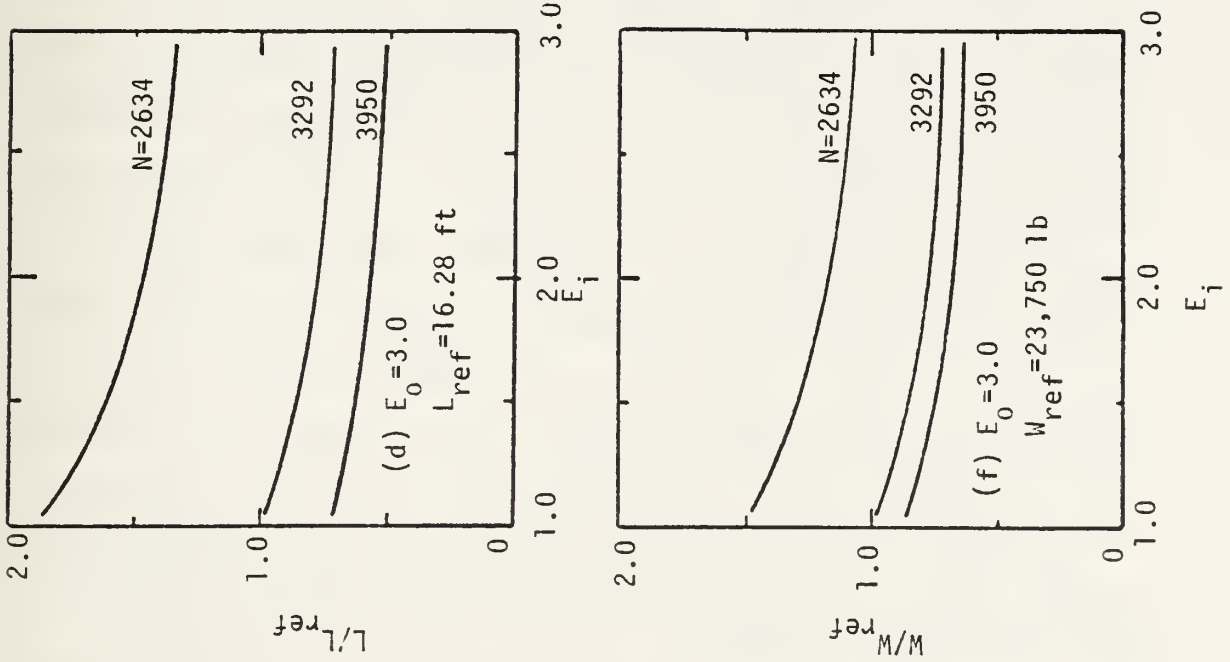


Figure 11 (continued). Variations of bundle length, volume, and weight. Baseline heat duty with cooling water velocity of 8 ft/s; (d)-(f) external enhancement factor  $E_0 = 3.0$ .

Comparing Figures a and d, b and e, and c and f, it will be seen that bundle length, volume, and weight may all be reduced through enhancement ( $E_i = E_o = 3.0$ ) by factors of about 38% with the number of tubes held constant at the baseline value of 3292.

An increase in the number of tubes will require an increase in the bundle diameter while allowing, at the same time, a decrease in the tube length necessary to sustain the given heat load. These two effects are in opposition as regards bundle volume and weight and in the case of no enhancement (Figs. 11a-11c,  $E_i = 1.0$ ) the decrease in length (about 27%) is sufficient to allow decreases in both volume (20%) and weight (13%). At high levels of internal enhancement, however, the allowable length reduction due to additional tubes is somewhat less and although volume reduction is still obtained the trend in bundle weight decreases and is eventually reversed with  $E_i = 2.5$  and  $E_o = 1$ . For example, the length reduction accompanying a 20% increase in tubes is about 11%, with a volume reduction of 5.4% and a negligible change in weight. At even higher values of  $E_i$  it is seen that a 20% increase in tubes leads to an increase in bundle weight - an effect that is opposite to that for the situation without enhancement. Reversals in trends, such as these, are often impossible to predict if steam-side interaction effects are not taken into account.

If, on the other hand, it is desirable to reduce the number of tubes (for space considerations or to reduce cooling water flow rate, for example) a 20% decrease in the number of tubes will give a 10% reduction in bundle diameter. Without enhancement, this would require increases in length, volume, and weight of 90%, 70%, and 26%, respectively. If enhancement ( $E_i = E_o = 3.0$ ) is utilized, however, the percentage increases in length and volume are only 15% and 6% while the bundle weight is decreased by about 7%. Thus, enhancement can allow condenser modifications for "packaging" purposes that might otherwise be impossible.

In the examples cited in Fig. 11, the condenser cooling water velocity has been held constant at 8.0 ft/s. For variable bundle diameters, the cooling water flow rate must therefore change in proportion with the number of tubes. These variations and constraints are used here for illustrative purposes and they represent only a few of the cases under consideration. It should also be remarked that here we have made only minor mention of the changes in cooling water head loss and pumping power that accompany the many variations shown in Figs. 8-11. Obviously, the relative merits of adjustments such as these depend upon the premiums to be placed upon the costs and benefits. If increases in bundle diameter can be tolerated, for instance, there are significant payoffs to be had in reductions in length, volume, weight, and cooling water pumping power.

## SUMMARY

The authors wish to again remind the reader that these calculations are most trustworthy when viewed as bases for comparisons. The extremely complex nature of the flow and heat transfer in condenser bundles leaves much to be accomplished through further research. It is hoped that, with these precautions, the utility of a code such as MORCON has been illustrated. It is expected that future design comparisons such as these will be expedited by the development of a numerical optimization code, based upon MORCON, to alleviate the serendipity required to optimize such complex phenomena as condenser bundles.

In closing, it is to be emphasized that several other performance factors and design variables, not mentioned here, are under study. The various tube-side and shell-side pressure drop legacies associated with enhancement are calculated and these constitute some of the "costs" to be balanced against the benefits of enhancement. A paramount factor yet to be understood is the extent to which fouling offsets the benefits of enhancement. Other design variables, such as tube material, tube diameter and wall thickness, condenser steam inlet pressure, and cooling water velocity and flow rate are under consideration. A change to titanium tubes will, in itself, generate a reduction in bundle weight by a factor of approximately 3 because of reduced metal density

and tube wall thicknesses. With all design variables left to vary within reasonable constraints, it is expected that improvements in tube bundle weight and volume may be realized in excess of those cited here and with acceptable penalties in terms of pressure drops and pumping powers.

#### CONCLUDING REMARKS

On the basis of work reported here and elsewhere, it is apparent that the continued advancement of the technology associated with surface condensers will require improvements in the understanding and definition of the flow conditions on the two-phase multi-component side of the problem. Whereas the prediction of the performance of single tubes - with vapor-side conditions well defined - has seemed adequate in the past, this situation may be attributed to conservative design attitudes and to the fact that thermal resistances other than those on the vapor side have dominated the overall thermal circuit. Advanced condenser designs that seek optimal performance (minimum weight, maximum efficiency, etc.) will require a level of analytical sophistication that exceeds present-day standards.

A case in fact is that in which enhanced tubes are contemplated for use in condenser bundles. The prediction of condenser performance based upon single-tube theory and experiment cannot be expected to be reliable. Overall condenser

performance may exceed or fall short of such predictions depending upon the selection of the tubes themselves as well as their geometry and location in the condenser bundle.

Computer-based analyses can be used to advantage in the estimation of the tube-to-tube variation of flow conditions within a condenser bundle. In this report, a condenser computer code of moderate complexity has been described and its use has been demonstrated in several sample cases. The results of these computer experiments have served to illustrate the importance of internal detail in the prediction of the performance of condensers utilizing enhanced tubes. In addition, these studies have shown that judicious use of enhanced tubes can lead to considerable improvements in condenser performance as well as the realization of heretofore unattainable design options.

## LIST OF REFERENCES

1. Fujii, T., Honda, H., and Oda, K., "Condensation of Steam on a Horizontal Tube - the Influence of Oncoming Velocity and Thermal Condition at the Tube Wall," Proc., 18th Nat'l. Heat Transfer Conference, San Diego, Aug., 1979, ASME, pp. 35-43.
2. Mayhew, V.R., Griffiths, D.J., and Phillips, J.W., "Effect of Vapour Drag on Laminar Film Condensation on a Vertical Surface," Proc. Inst. Mech. Engrs., 1965-66, v. 180, pt. 35, pp. 280-287.
3. Nicol, A.A., Bryce, A., and Ahmed, A.S.A., "Condensation of Steam on a Cylinder in Vapour Crossflow," Proc. 6th Int'l. Heat Transfer Conf., paper no. C54, Toronto, 1978.
4. Power Condenser Heat Transfer Technology, eds. Marto, P.J. and Nunn, R.H., Hemisphere, New York, 1981, pp. 193-270.
5. Nusselt, W., "Die Oberflachen-Kondensation des Wasserdampfes", VDI Zeitung, Vol. 60, 1916, pp. 541-546, and pp. 569-575.
6. Nobbs, D.W., "The Effect of Downward Vapour Velocity and Inundation on the Condensation Rates on Horizontal Tubes and Tube Banks," Ph.D. Dissertation, Univ. of Bristol, April, 1975.
7. Eissenberg, D.M., "An Investigation of the Variables Affecting Steam Condensation on the Outside of a Horizontal Tube Bundle," Ph.D. Dissertation, Univ. of Tennessee, December, 1972.
8. Davidson, B.J., and Rowe, M., "Simulation of Power Plant Condenser Performance by Computational Methods," in Power Condenser Heat Transfer Technology, Hemisphere, New York, 1981, pp. 17-49.
9. Grant, I.D.R., and Osmeat, B.D.J., "The Effect of Condensate Drainage on Condenser Performance," NEL Report No. 350, National Engineering Lab, Glasgow, 1968.
10. Kern, D.Q., "Mathematical Development of Loading in Horizontal Condensers," J. Am. Inst. Chem. Engrs., v. 4, no. 2, 1958, pp. 157-160.
11. Brickell, G.M., "Potential Problem Areas in Simulating Condenser Performance," in Power Condenser Heat Transfer Technology, Hemisphere, New York, 1981, pp. 51-61.

12. Croix, J.M. and Liegeois, A., "Condensation on a Horizontal Tube Bundle," Report No. TT/SETRE/78-3-B/JMC, ALI, Centre Nucleaire, Grenoble, France, March, 1978.
13. Young, E.H., Withers, J.G. and Lampert, W.B., "Heat Transfer Characteristics of Corrugated Tubes in Steam Condensing Applications," AIChE Paper No. 3, 15th National Heat Transfer Conference, San Francisco, CA., August, 1975.
14. Naval Boiler and Turbine Laboratory Test T-235, DLG-6 Class Propulsion Machinery, by Foti, J.J., 15 Jan 1960.
15. Chisholm, D., "Modern Developments in Marine Condensers: Noncondensable Gases: An Overview," in Power Condenser Heat Transfer Technology, Hemisphere, New York, 1981, pp. 95-142.
16. Cunningham, J., "The Effect of Noncondensable Gases on Enhanced Surface Condensation," ibid., pp. 353-366.
17. Standards for Steam Surface Condensers, Heat Exchange Institute, New York, 1970.
18. Recommended Practice for the Design of Surface Type Steam Condensing Plant, British Electrical and Allied Manufacturers' Assn., London, 1967.
19. Coit, R.L., "A Designer's Approach to Surface Condenser Venting and Deaeration," in Power Condenser Heat Transfer Technology, Hemisphere, New York, 1981, pp. 163-180.
20. Comment by Wenzel, L.A., ibid., p. 182.
21. ORCON1: A Fortran Code for the Calculation of a Steam Condenser of Circular Cross Section, OLNL-TM-4248, by Hafford, J.A., Oak Ridge National Laboratory, Tennessee, July, 1973.
22. Chilton, T.H., and Colburn, A.P., "Mass Transfer (Absorption) Coefficients," Ind. Eng. Chem., v. 26: 1184, 1934.
23. Butterworth, D., "Inundation Without Vapor Shear," in Power Condenser Heat Transfer, Hemisphere, New York, 1981, pp. 271-277.
24. Eissenberg, D.M. and Noritake, H.M., "Computer Model and Correlations for Prediction of Horizontal Tube Condenser Performance in Seawater Distillation Plants," Report ONRL-TM-2972, Oak Ridge National Laboratory, Tennessee, Oct. 1970.

25. Korodense Bulletin 4020, Wolverine Division, Decatur, Ala., 5 Jan., 1976.
26. Technical Memorandum 3, Yorkshire Imperial Metals, LTD., Leeds, England.







## FILE: MCRCON FORTRAN A NAVAL POSTGRADUATE SCHOOL

## FILE: MCRCON FORTRAN A NAVAL POSTGRADUATE SCHOOL

```

CCCC  HACCSV = HACCV
      VNCSSV = VNCSC
      LVCSSV = LVCSC
      CALL COOLINGDE LPC1
      FCBMAT (1,1,1)HCCOLEX DONE)
      FCF = 1.07001
      FCF = 1.07001 / ADJF * SECFLG
      ECF = 1.07001 / SECFLG * 100
      CALL COOLINGDE (VNCSC1,100,1,0
      FCF = 1.07001 / EXFCR1 WSI1 ALST. IWS,ILNG,INSTN,EXFCR1
      YCA = 1.07001 / ALST. IWS,ILNG,INSTN,EXFCR1
      HACCSV = HACCV
      LVCSSV = LVCSC
      VNCSSV = VNCSC
      IWS,ILNG,INSTN,EXFCR1 SECFLG
      IWS,ILNG,INSTN,EXFCR1 / 100
      GC 10,20C
      CCONTINUE TAC SCLADJF SECFLG
      XFCR1 = 1.04001 XFCR1, 1W1, TNOC
      HAC = WAC
      CALL COOLINGDE LFC,YEL2(NERR)
      TAC = TAC / SECFLG
      GC 10,10
      REUPN TUBE ROWS IN CNDNSR, WHICH EXCEEDS PROGRAM DIMM
      10000 FCNAMT = 10.000, INPUT ERRCA, INCORRECT NO. OF ROWS IN CONDENSER.
      10100 FCNAMT = 10.000, INPUT ERRCA, INCORRECT NO. OF ROWS IN CONDENSER.
      10200 FCNAMT = 10.000, TUBE ROWS IN COOLER, WHICH EXCEEDS PROGRAM DIMM
      10300 FCNAMT = 10.000, INPUT ERRCA, INCORRECT NO. OF ROWS IN COOLER.
      10400 FCNAMT = 10.000, INPUT ERRCA, INCORRECT NO. OF ROWS IN COOLER.
      * ACTUAL TUBES IN CONDENSER. #6.1, #7.4, T#0
      * ACTUAL TUBES IN COOLER.
      END

```

```

      WSI1MAX = WSI1
      WSI1MIN = WSI1
      20 WSI1MIN = ALST
      30 CCONTINUE TAC, IWS,ILNG,INSTN,EXFCR1 GC TO 70
      IF (INSTN = F0,0) GC TO 70
      IF (IWS = -1.07010000, WSI1MAX,WSI1MIN,EXFCR1
      WRITE (2,10001 WSI1MAX,WSI1MIN,EXFCR1
      CONTINUE
      40
      ***** ADJUSTMENT FOR INLET STEAM
      *****
      DELWP = ABS(WSI1MAX-WSI1MIN)
      K21L0 = XIF(WSI1MAX,IWS,EXFCR1,-1.0,XIN,YN,WI)
      K21L1 = XIF(WSI1MIN,IWS,EXFCR1,-1.0,XIN,YN,WI)
      DELPK = WSI1MAX * COLD / IWS
      DELWPK = DELWP / 2.0
      K21P1 = XIF(WSI1MAX,IWS,EXFCR1,-1.0,XIN,YN,WI)
      K21P2 = XIF(WSI1MIN,IWS,EXFCR1,-1.0,XIN,YN,WI)
      GC TO 6.1
      WSI1MAX = 0.700 * COLD / IWS
      WSI1MIN = 0.630 * COLD / IWS
      DELWPK = DELWP / 2.0
      ***** ADJUSTMENT FOR TUBE LENGTH
      *****
      C21L0 = ABS(STPA-ALST)
      ALSTLD = ABS(STPA-ALST)
      C21L1 = XIF(ALST,IWS,ILNG,EXFCR1,1.0,XIN,YN,WI)
      C21L2 = ALSTLD * 0.01 / ILNG
      IF (DELA = G1,DELAP,DELA = DELAP / 2.0
      ALST = ALSTLD * DELA
      GC TO 10,11
      C21L3 = ABS(STPA-ALST) * 0.01 / ILNG
      K21L3 = XIF(STPA-ALST,0.01 / ILNG,0.001 ALST,WI,EXFCR1
      C21L4 = ABS(STPA-ALST) * 0.01 / ILNG
      K21L4 = XIF(STPA-ALST,0.01 / ILNG,0.001 ALST,WI,EXFCR1
      CONTINUE
      60
      ***** ADJUSTMENT FOR TUBE LENGTH
      *****
      C21L5 = ABS(STPA-ALST)
      ALSTLD = ABS(STPA-ALST)
      C21L6 = XIF(ALST,IWS,ILNG,EXFCR1,1.0,XIN,YN,WI)
      C21L7 = ALSTLD * 0.01 / ILNG
      IF (DELA = G1,DELAP,DELA = DELAP / 2.0
      ALST = ALSTLD * DELA
      GC TO 10,11
      C21L8 = ABS(STPA-ALST) * 0.01 / ILNG
      K21L8 = XIF(STPA-ALST,0.01 / ILNG,0.001 ALST,WI,EXFCR1
      C21L9 = ABS(STPA-ALST) * 0.01 / ILNG
      K21L9 = XIF(STPA-ALST,0.01 / ILNG,0.001 ALST,WI,EXFCR1
      CONTINUE
      70
      ***** ADJUSTMENT FOR TUBE LENGTH
      *****
      C21L10 = ABS(STPA-ALST)
      ALSTLD = ABS(STPA-ALST)
      C21L11 = XIF(ALST,IWS,ILNG,EXFCR1,1.0,XIN,YN,WI)
      C21L12 = ALSTLD * 0.01 / ILNG
      IF (DELA = G1,DELAP,DELA = DELAP / 2.0
      ALST = ALSTLD * DELA
      GC TO 10,11
      C21L13 = ABS(STPA-ALST) * 0.01 / ILNG
      K21L13 = XIF(STPA-ALST,0.01 / ILNG,0.001 ALST,WI,EXFCR1
      C21L14 = ABS(STPA-ALST) * 0.01 / ILNG
      K21L14 = XIF(STPA-ALST,0.01 / ILNG,0.001 ALST,WI,EXFCR1
      CONTINUE
      80
      ***** ADJUSTMENT FOR TUBE LENGTH
      *****
      C21L15 = ABS(STPA-ALST)
      ALSTLD = ABS(STPA-ALST)
      C21L16 = XIF(ALST,IWS,ILNG,EXFCR1,1.0,XIN,YN,WI)
      C21L17 = ALSTLD * 0.01 / ILNG
      IF (DELA = G1,DELAP,DELA = DELAP / 2.0
      ALST = ALSTLD * DELA
      GC TO 10,11
      C21L18 = ABS(STPA-ALST) * 0.01 / ILNG
      K21L18 = XIF(STPA-ALST,0.01 / ILNG,0.001 ALST,WI,EXFCR1
      C21L19 = ABS(STPA-ALST) * 0.01 / ILNG
      K21L19 = XIF(STPA-ALST,0.01 / ILNG,0.001 ALST,WI,EXFCR1
      CONTINUE
      90
      ***** ADJUSTMENT FOR TUBE LENGTH
      *****
      C21L20 = ABS(STPA-ALST)
      ALSTLD = ABS(STPA-ALST)
      C21L21 = XIF(ALST,IWS,ILNG,EXFCR1,1.0,XIN,YN,WI)
      C21L22 = ALSTLD * 0.01 / ILNG
      IF (DELA = G1,DELAP,DELA = DELAP / 2.0
      ALST = ALSTLD * DELA
      GC TO 10,11
      C21L23 = ABS(STPA-ALST) * 0.01 / ILNG
      K21L23 = XIF(STPA-ALST,0.01 / ILNG,0.001 ALST,WI,EXFCR1
      C21L24 = ABS(STPA-ALST) * 0.01 / ILNG
      K21L24 = XIF(STPA-ALST,0.01 / ILNG,0.001 ALST,WI,EXFCR1
      CONTINUE
      100
      ***** ADJUSTMENT FOR TUBE LENGTH
      *****
      C21L25 = ABS(STPA-ALST)
      ALSTLD = ABS(STPA-ALST)
      C21L26 = XIF(ALST,IWS,ILNG,EXFCR1,1.0,XIN,YN,WI)
      C21L27 = ALSTLD * 0.01 / ILNG
      IF (DELA = G1,DELAP,DELA = DELAP / 2.0
      ALST = ALSTLD * DELA
      GC TO 10,11
      C21L28 = ABS(STPA-ALST) * 0.01 / ILNG
      K21L28 = XIF(STPA-ALST,0.01 / ILNG,0.001 ALST,WI,EXFCR1
      C21L29 = ABS(STPA-ALST) * 0.01 / ILNG
      K21L29 = XIF(STPA-ALST,0.01 / ILNG,0.001 ALST,WI,EXFCR1
      CONTINUE
      110
      ***** ADJUSTMENT FOR TUBE LENGTH
      *****
      C21L30 = ABS(STPA-ALST)
      ALSTLD = ABS(STPA-ALST)
      C21L31 = XIF(ALST,IWS,ILNG,EXFCR1,1.0,XIN,YN,WI)
      C21L32 = ALSTLD * 0.01 / ILNG
      IF (DELA = G1,DELAP,DELA = DELAP / 2.0
      ALST = ALSTLD * DELA
      GC TO 10,11
      C21L33 = ABS(STPA-ALST) * 0.01 / ILNG
      K21L33 = XIF(STPA-ALST,0.01 / ILNG,0.001 ALST,WI,EXFCR1
      C21L34 = ABS(STPA-ALST) * 0.01 / ILNG
      K21L34 = XIF(STPA-ALST,0.01 / ILNG,0.001 ALST,WI,EXFCR1
      CONTINUE
      120
      ***** ADJUSTMENT FOR TUBE LENGTH
      *****
      C21L35 = ABS(STPA-ALST)
      ALSTLD = ABS(STPA-ALST)
      C21L36 = XIF(ALST,IWS,ILNG,EXFCR1,1.0,XIN,YN,WI)
      C21L37 = ALSTLD * 0.01 / ILNG
      IF (DELA = G1,DELAP,DELA = DELAP / 2.0
      ALST = ALSTLD * DELA
      GC TO 10,11
      C21L38 = ABS(STPA-ALST) * 0.01 / ILNG
      K21L38 = XIF(STPA-ALST,0.01 / ILNG,0.001 ALST,WI,EXFCR1
      C21L39 = ABS(STPA-ALST) * 0.01 / ILNG
      K21L39 = XIF(STPA-ALST,0.01 / ILNG,0.001 ALST,WI,EXFCR1
      CONTINUE
      130
      ***** SUBROUTINE ZEROL(A,I)
      N=I/4
      D=I-1,N4
      1
      RETURN
      END
      ***** SUBROUTINE ADJUST CORRECTS EITHER INPUT STEAM OR TYPE LENGTH
      * WHICH GIVES PREDICTED EXIT STREAM FRATION FROM THE COOLER
      * AS A PERCENT OF STREAM INPUT.
      JAH
      4/70
      ***** DIMENSION XIN,ILNG,YIN,EXFCR,EXFCR1,ALST,ILNG,INSTN,EXFCR1
      * IF (ABS(XIN-EXFCR1) .GT. 0.001)
      * XIN = XIN - EXFCR1
      * ALST = ALST - EXFCR1
      * ALSTPK = 0.0
      * ALSTMN = 0.0
      * 10
      CONTINUE
      EXFCR = EXFCR1 / 100.
      IF (EXFCR .LT. EXFCR1) GO TO 20
      ALSTMN = ALST
      20
      ***** SUBROUTINE CCOLEX CIRCB 99 -- 360/CS 12/20/68
      CCC
      E

```























Appendix B. Input Data Deck for Baseline Design

4 MORCCN REPORT, BASELINE CASE, SMOOTH TUBE, 8/05/82  
1646 6.00 1.350 1.350 .0650 17.0 0 0  
4046762: 0.0 0.035 66.1 .000329 1.00  
AIR 6: 0. 1.0 0.0 0.05 0 0 1.0  
189002: 33.7 1.3373 0.05 38.000 1.00  
1.000 58.00 6.000 0.000  
1



## Appendix C. Summary and Detailed Output for Baseline Design

FILE: M C A NAVAL POSTGRADUATE SCHOOL

PAGE 001

1 CASE IDENTIFICATION AND NOTES \*\*\* MORCON REPORT. BASELINE CASE. SMOOTH TUBE. 8/05/82  
 CIRCULAR CONDENSER INPUT DATA

CASE	REF	NAME	DESCRIPTION	VAL	UNIT	VAL	UNIT	VAL	UNIT	VAL	UNIT	VAL	UNIT	VAL	UNIT	VAL	UNIT	VAL	UNIT
0	CARC 1	MCFCN REFCN	SMOOTH CASE, SMOOTH TUBE.	8/05/82	XW		KW		XW		KW		NRWS	NRWS					
0	CARC 2	ANT	PA CLR	SOO	SDMIN	0.0	F0UL	0.6250	ENH1	0.0650	ENH1	0.17	0.00	0					
0	CARC 3	164.	WB1	6.00	ST1	1.50	F0UL	0.6250	ENH1	0.0650	ENH1	0.17	0.00	0					
0	CARC 4	4046763.	SECFL	6.0	0.02500	6.00	100C	0.0033	FOAVE	1.000	EXITFR	0.000	INSTM	0					
C	CARC 5	GAS	HFCDFL	0.0	0.02500	6.0	RADFLG	0.000	FOAVE	1.000	INSTM	0	ITRAN	1	FLOAT	1	IPNCH		
0	CARC 6	AIR	ALST	0.0	0.05000	0.0	0.05000	0.000	ENHF	0.000	ENHF	0.0	ENHF	0					
0	CARC 7	18903.	TEBSA	133.70	STSAT1	1.00	ALST	0.000	ENHF	1.000	ENHF	0.0							
C	CARC 8	ENH1	TEBSA	133.70	STSAT1	1.00	ALST	0.000	ENHF	1.000	ENHF	0.0							
C	CARC 9	1VAF	TEBSA	133.70	STSAT1	1.00	ALST	0.000	ENHF	1.000	ENHF	0.0							
C	CARC 10	1VAF	TEBSA	133.70	STSAT1	1.00	ALST	0.000	ENHF	1.000	ENHF	0.0							
1	INPUT DINE OKEYNOUCS NUMBER IN CONDENSER ON SHELL SIDE HAS FALLEN BELOW 100. RENC = 0.917591E+02 SECTOR 6 ROW 28 0*** STEAM VELOCITY IN FIRST ROW OF COOLER TUBES EXCEEDS MAX ALLOWABLE. VELC(1) = 0.17068E+03 C COOLER DIMENSIONS ADJUSTED TO LOWER STEAM VELOCITY. VELC(1) = 0.14889E+03 C OKEYNOUCS NUMBER IN COOLER ON SHELL SIDE HAS FALLEN BELOW 100. RENO = 0.937834E+02 SECTOR 7 ROW 25 C COOLER CONE 0 ALTOLO = 38.000 XTRFL = 0.0000 ALST = 37.909 C SECALC CONE STEAM VELOCITY IN FIRST ROW OF COOLER TUBES EXCEEDS MAX ALLOWABLE. VELC(1) = 0.17525E+03 C COOLER DIMENSIONS ADJUSTED TO LOWER STEAM VELOCITY. VELC(1) = 0.14745E+03 C OKEYNOUCS NUMBER IN COOLER ON SHELL SIDE HAS FALLEN BELOW 100. RENO = 0.527462E+02 SECTOR 7 ROW 26 C COOLER CONE 0 ALTOLO = 37.909 XTRFL = 0.0000 ALST = 37.821 C SECALC CONE STEAM VELOCITY IN FIRST ROW OF COOLER TUBES EXCEEDS MAX ALLOWABLE. VELC(1) = 0.17974E+03 C COOLER DIMENSIONS ADJUSTED TO LOWER STEAM VELOCITY. VELC(1) = 0.14560E+03 C OKEYNOUCS NUMBER IN COOLER ON SHELL SIDE HAS FALLEN BELOW 100. RENO = 0.786101E+02 SECTOR 7 ROW 25 C COOLER CONE 0 ALTOLO = 37.821 XTRFL = 0.0000 ALST = 37.391 C SECALC CONE STEAM VELOCITY IN FIRST ROW OF COOLER TUBES EXCEEDS MAX ALLOWABLE. VELC(1) = 0.20197E+03 C COOLER DIMENSIONS ADJUSTED TO LOWER STEAM VELOCITY. VELC(1) = 0.14473E+03 C OKEYNOUCS NUMBER IN COOLER ON SHELL SIDE HAS FALLEN BELOW 100. RENO = 0.14473E+03 C COOLER CONE 0 ALTOLO = 37.391 XTRFL = 0.0008 ALST = 37.463 C SECALC CONE STEAM VELOCITY IN FIRST ROW OF COOLER TUBES EXCEEDS MAX ALLOWABLE. VELC(1) = 0.19813E+03 C COOLER DIMENSIONS ADJUSTED TO LOWER STEAM VELOCITY. VELC(1) = 0.14615E+03 C OKEYNOUCS NUMBER IN COOLER ON SHELL SIDE HAS FALLEN BELOW 100. RENO = 0.14615E+03 C COOLER CONE 0 ALTOLO = 37.463 XTRFL = 0.0008 ALST = 37.489 C SECALC CONE STEAM VELOCITY IN FIRST ROW OF COOLER TUBES EXCEEDS MAX ALLOWABLE. VELC(1) = 0.19673E+03 C COOLER DIMENSIONS ADJUSTED TO LOWER STEAM VELOCITY. VELC(1) = 0.14710E+03																		

C COOLEX CONE  
 Q SECAL CCNE 37.469 XTRFL = 0.0006 ALST = 37.497  
 Q\*\*\* STEAM VELOCITY IN FIRST ROW OF COOLER TUBES EXCEEDS MAX ALLOWABLE. VELC(1) = 0.19634E+03  
 C COOLER DIMENSIONS ADJUSTED TO LOWER STREAM VELOCITY. VELC(1) = 0.14681E+03  
 C COOLEX CONE 24ROWS CF TUBES 4.012TUBES PER ROW  
 Q 6 ALTCIO = 37.497 XTRFL = 0.0006 ALST = 37.564  
 C SECAL CCNE 0\*\*\* STEAM VELOCITY IN FIRST ROW OF COOLER TUBES EXCEEDS MAX ALLOWABLE. VELC(1) = 0.19287E+03  
 O COOLER DIMENSIONS ADJUSTED TO LOWER STREAM VELOCITY. VELC(1) = 0.15022E+03  
 C 25ROWS CF TUBES 3.85TUBES PER ROW  
 CHEYNOLDS NUMBER IN COOLER ON SHELL SIDE HAS FALLEN BELOW 100. RENO = 0.889950E+02 SECTOR 7 ROW 25  
 C 7 ALTCIO = 37.564 XTRFL = 0.0002 ALST = 37.500  
 C SECAL CCNE 0\*\*\* STEAM VELOCITY IN FIRST ROW OF COOLER TUBES EXCEEDS MAX ALLOWABLE. VELC(1) = 0.19621E+03  
 C COOLER DIMENSIONS ADJUSTED TO LOWER STREAM VELOCITY. VELC(1) = 0.14671E+03  
 C 8 ALTCIO = 37.500 XTRFL = 0.0006 ALST = 37.504  
 C SECAL CCNE 0\*\*\* STEAM VELOCITY IN FIRST ROW OF COOLER TUBES EXCEEDS MAX ALLOWABLE. VELC(1) = 0.19594E+03  
 O COOLER DIMENSIONS ADJUSTED TO LOWER STREAM VELOCITY. VELC(1) = 0.14651E+03  
 C COOLEX CONE CONVERGENCE CRITERIA MET FOR EXIT STEAM  
 C COOLER EXIT STEAM FRAC 0.0005 ACTUAL TUBES IN CONDENSER 1546.7 ACTUAL TUBES IN COOLER 96.3  
 C COOLER CASE. SMOOTH TUBE. 8/05/82 SUMMARY OF RESULTS  
 C COOLER EXIT STEAM FRAC 0.0005 ACTUAL TUBES IN CONDENSER 1546.7 ACTUAL TUBES IN COOLER 96.3  
 AREA AVERAGE BACK CALC.  
 LCG MEAN PRESSURE TEMP. STEAM VELOCITY TUBE SPACING TUBE FRACTION REMOVED SURFACE.  
 671L/HR/SC.FT. DELT TEMP. DROPOUT FT/SEC. INLET FT OUTLET FT PERCENT SQ.FT.  
 OEG.F. OEG.F. LBS/SCIN. DEG.F. DEG.F. DEG.F. DEG.F. DEG.F. DEG.F. DEG.F. DEG.F.  
 CCNENSER 53.3.7.3 35.9.6.9 0.0700 120.75 54.54 1.250 94.15 182.5716 9510.04  
 COOLER 4.96.7.3 32.4.6.32 0.0593 125.59.48 54.54 1.250 94.15 182.5716 9510.04  
 COVERALL 520.266 32.4.660 0.1733 34.36.5 3.68 1.350 5.85 192.4261 10100.90  
 COOLING BUNDLE 0.1.1 FT. 4.15 INSIDE VOL 0.149 FT. 0.33 BUNDLE LENGTH. FT. NUMBER OF RADIAL TUBE ROWS 30.  
 COOLER FEATH FT. 1.51 COOLER WIDTH. FT. 0.33 EXIT NON-CONEABLES. PERCENT OF TOTAL EXIT FLOW 252.73  
 Q EXIT STEAM. PERCENT OF INPUT 5.272E-02  
 AVG ERINE TEMPS 116.4253 STEAM TO CONDENSER LBS/HR 189003.  
 CONNENSER 11.008 113.2591 COOLANT TO BUNDLE COOLANT VELOCITY 400.6762.  
 COOLER 6.1002 113.2401 COOLANT FROM CONDENSER 8.0000F/S  
 OVERALL 6.6.1007 116.3401 CONDENSATE FROM CONDENSER 179240.  
 C LTCNC2 LPPONG 0.07012 UPCCOL DL.TOT2 UPAVG 9654.  
 C BUNL2F FUNVCL 81UNW1 RETUD FRIFAC MOLOSS PMPMPR  
 1.875E+01 2.536E+02 2.735E+04 2.099E+04 2.427E-02 2.194E+01 4.485E+01

## GLOSSARY OF TERMS USED IN THE DETAILED OUTPUT

FIRST COLUMN INDICATES RCM NUMBER. INTEGER A DESIGNATES SECTOR.  
 STAT MIXTURE TEMPERATURE ENTERING THE ROW. DEG F  
 PHX MIXTURE PRESSURE. PSIA  
 WS STREAM RECHT FLOW RATE TO ROW. LB/HR  
 VEL STREAM VELOCITY AT MINIMUM CROSS SECTION. FT/SEC  
 RC WEIGHT FRACTION OF NONCONDENSABLE GASES  
 UN OVERALL HEAT TRANSFER COEFFICIENT FOR THE "MEAN" TUBE.  
 FTU/HR-FT\*\*2-OEG F

FILE: P

A NAVAL POSTGRADUATE SCHOOL

PAGE 003

S<sub>H</sub>NF CONDENSATE FILM HEAT TRANSFER COEFFICIENT. 8TU/HR-FT<sup>2</sup>-DEG F  
 S<sub>H</sub>F TUBE SIDE HEAT TRANSFER COEFFICIENT. 8TU/HR-FT<sup>2</sup>-DEG F  
 1/R<sub>CUT</sub> STEAM SIDE HEAT TRANSFER COEFFICIENT (CONDENSATE AND GAS).

R<sub>EN</sub>CS REYNOLDS NUMBER AT MINIMUM CROSS SECTION  
 LOCAL F<sub>E</sub>A LOCAL F<sub>E</sub>A FRICTION FACTOR AT CURRENT ROW. LB/HR

SF FRICTION FACTOR OF VAPOR AT INLET TEMPERATURE. DEG F

CFD CIRCULATING WATER OUTLET TEMPERATURE. DEG F

COEF COEFFICIENT OF NON-CONDENSABLE FILM.

PTU/HR-FT<sup>2</sup>-DEG F

ALNUF NUMBER OF COEF IN RCH

CUM CDFL CUMULATIVE PRESSURE DROP FROM ENTRANCE. IN. H<sub>2</sub>O

I. POKCON REPORT. BASELINE CASE, SMOOTH TUBE. 8/05/82

	ST <sub>N</sub> T <sub>A</sub>	FIXE	V <sub>L</sub>	R <sub>C</sub>	S <sub>H</sub> F	1/R <sub>CUT</sub>	T <sub>NPR</sub>	CUM DELP
0	1.3502E+02	2.4357E+00	3.1E+02	1.1942E+02	1.7824E-04	4.0250E+03	4.0236E+03	4.0236E+03
1	1.3515E+02	2.4359E+00	3.1E+02	1.1903E+02	1.7824E+00	4.0250E+03	3.3933E+03	3.3933E+03
2	1.3528E+02	2.4362E+00	3.1E+02	1.1864E+02	1.7824E-04	4.0250E+03	3.9215E+03	3.9215E+03
3	1.3541E+02	2.4364E+00	3.1E+02	1.1825E+02	1.7824E+00	4.0250E+03	3.9215E+03	3.9215E+03
4	1.3554E+02	2.4367E+00	3.1E+02	1.1786E+02	1.7824E-04	4.0250E+03	3.9215E+03	3.9215E+03
5	1.3567E+02	2.4370E+00	3.1E+02	1.1747E+02	1.7824E+00	4.0250E+03	3.9215E+03	3.9215E+03
6	1.3580E+02	2.4373E+00	3.1E+02	1.1708E+02	1.7824E-04	4.0250E+03	3.9215E+03	3.9215E+03
7	1.3593E+02	2.4376E+00	3.1E+02	1.1669E+02	1.7824E+00	4.0250E+03	3.9215E+03	3.9215E+03
8	1.3607E+02	2.4379E+00	3.1E+02	1.1630E+02	1.7824E-04	4.0250E+03	3.9215E+03	3.9215E+03
9	1.3620E+02	2.4382E+00	3.1E+02	1.1591E+02	1.7824E+00	4.0250E+03	3.9215E+03	3.9215E+03
10	1.3634E+02	2.4385E+00	3.1E+02	1.1552E+02	1.7824E-04	4.0250E+03	3.9215E+03	3.9215E+03
11	1.3647E+02	2.4388E+00	3.1E+02	1.1513E+02	1.7824E+00	4.0250E+03	3.9215E+03	3.9215E+03
12	1.3660E+02	2.4391E+00	3.1E+02	1.1474E+02	1.7824E-04	4.0250E+03	3.9215E+03	3.9215E+03
13	1.3674E+02	2.4394E+00	3.1E+02	1.1435E+02	1.7824E+00	4.0250E+03	3.9215E+03	3.9215E+03
14	1.3687E+02	2.4397E+00	3.1E+02	1.1396E+02	1.7824E-04	4.0250E+03	3.9215E+03	3.9215E+03
15	1.3700E+02	2.4400E+00	3.1E+02	1.1357E+02	1.7824E+00	4.0250E+03	3.9215E+03	3.9215E+03
16	1.3713E+02	2.4403E+00	3.1E+02	1.1318E+02	1.7824E-04	4.0250E+03	3.9215E+03	3.9215E+03
17	1.3726E+02	2.4406E+00	3.1E+02	1.1279E+02	1.7824E+00	4.0250E+03	3.9215E+03	3.9215E+03
18	1.3739E+02	2.4409E+00	3.1E+02	1.1240E+02	1.7824E-04	4.0250E+03	3.9215E+03	3.9215E+03
19	1.3753E+02	2.4412E+00	3.1E+02	1.1191E+02	1.7824E+00	4.0250E+03	3.9215E+03	3.9215E+03
20	1.3766E+02	2.4415E+00	3.1E+02	1.1152E+02	1.7824E-04	4.0250E+03	3.9215E+03	3.9215E+03
21	1.3780E+02	2.4418E+00	3.1E+02	1.1113E+02	1.7824E+00	4.0250E+03	3.9215E+03	3.9215E+03
22	1.3793E+02	2.4421E+00	3.1E+02	1.1074E+02	1.7824E-04	4.0250E+03	3.9215E+03	3.9215E+03
23	1.3806E+02	2.4424E+00	3.1E+02	1.1035E+02	1.7824E+00	4.0250E+03	3.9215E+03	3.9215E+03
24	1.3820E+02	2.4427E+00	3.1E+02	1.1096E+02	1.7824E-04	4.0250E+03	3.9215E+03	3.9215E+03
25	1.3833E+02	2.4430E+00	3.1E+02	1.1057E+02	1.7824E+00	4.0250E+03	3.9215E+03	3.9215E+03
26	1.3846E+02	2.4433E+00	3.1E+02	1.1018E+02	1.7824E-04	4.0250E+03	3.9215E+03	3.9215E+03
27	1.3859E+02	2.4436E+00	3.1E+02	1.1079E+02	1.7824E+00	4.0250E+03	3.9215E+03	3.9215E+03
28	1.3873E+02	2.4439E+00	3.1E+02	1.1040E+02	1.7824E-04	4.0250E+03	3.9215E+03	3.9215E+03
29	1.3886E+02	2.4442E+00	3.1E+02	1.1001E+02	1.7824E+00	4.0250E+03	3.9215E+03	3.9215E+03
30	1.3899E+02	2.4445E+00	3.1E+02	1.1062E+02	1.7824E-04	4.0250E+03	3.9215E+03	3.9215E+03
1	1.3912E+02	2.4448E+00	3.1E+02	1.1023E+02	1.7824E-04	4.0250E+03	3.9215E+03	3.9215E+03















INITIAL DISTRIBUTION LIST

	No. Copies
1. Library, Code 0142 Naval Postgraduate School Monterey, California 93940	4
2. Office of Research Administration (012A) Naval Postgraduate School Monterey, California 93940	1
3. Professor Paul J. Marto, Code 69MX Naval Postgraduate School Monterey, California 93940	5
4. Professor Robert H. Nunn, Code 69Nn Naval Postgraduate School Monterey, California 93940	5
5. Mr. Raymond W. Kornbau, Code 2721 David W. Taylor Naval Ship Research and Development Center Annapolis, Maryland 21402	2
6. Dr. Frank Ventriglio, Code 05R Naval Sea Systems Command Department of the Navy Washington, D.C. 20362	1
7. Mr. Kurt Bredehorst, Code 5223 Naval Sea Systems Command Department of the Navy Washington, D.C. 20362	1
8. CDR. W. Marsh, Code 05DC3 Naval Sea Systems Command Department of the Navy Washington, D.C. 20362	1
9. Mr. M. Keith Ellingsworth Materials and Mechanics Branch Office of Naval Research Arlington, Virginia 22217	1





